

# **ME-411: Mechanics of Slender Structures**

## **Lecture Notes**

**Fall 2020**

Pedro M. Reis  
Flexible Structures Laboratory  
Institute of Mechanical Engineering  
Section of Mechanical Engineering  
École polytechnique fédérale de Lausanne  
Switzerland

**Note for the Students:** This is a living document that will be updated and expanded gradually, on a weekly basis, as the semester progresses. Updates with new content will be typically performed by Thursdays. We encourage you to make sure to have the latest version available on MOODLE.

**Last updated:** October 6, 2020.

**Acknowledgements:** We thank Bastien Aymon for help with the typing of these notes. A number of the members of the Flexible Structures Laboratory at EPFL worked, as a team effort, on preparing and polishing the material of this course. We are particularly grateful to: Paul Johanns, Arefeh Abbasi, Armelle Kaiser, Paul Grandgeorge, Tomohiko Sano, Tim Chen, Sam Poincloux, Dong Yan, and Matteo Pezzulla. The development, curation and organization of the present material has benefited from invaluable discussions and exchanges with a number of colleagues, especially: Basile Audoly, John Hutchinson, José Bico, Benoit Roman and Marcelo Dias.

**Copyright:** ©2020 Pedro M. Reis  
Section of Mechanical Engineering (SGM)  
School of Engineering (STI)  
École polytechnique fédérale de Lausanne  
Switzerland  
Email: [pedro.reis@epfl.ch](mailto:pedro.reis@epfl.ch)  
[Http://flexlab.epfl.ch](http://flexlab.epfl.ch)

**Colophon:** This document was typeset with the help of *KOMA-Script* and  $\LaTeX$  using the *kaobook* class. The source code of this book is available at: <https://github.com/fmarotta/kaobook>

# Contents

<b>Contents</b>	<b>iii</b>
<b>1 Beams: Traction, Bending, Torsion and Buckling</b>	<b>1</b>
1.1 Beam bending . . . . .	1
1.2 Torsion of rods and shafts . . . . .	5
1.3 Summary of stretching, bending and torsion of rods . . . . .	7
1.4 Castiglino's theorem . . . . .	8
1.5 Buckling of beams . . . . .	9
<b>2 Dimensional Analysis and Scalings</b>	<b>12</b>
2.1 Introduction . . . . .	12
2.2 Base dimensions and units . . . . .	12
2.3 Buckingham- $\Pi$ Theorem . . . . .	15
2.4 Summary of the recipe to solve a problem using dimensional analysis . . . . .	16
2.5 Extended dimensional analysis . . . . .	17
2.6 Physical similarity . . . . .	19
2.7 Scalings . . . . .	20
<b>3 Calculus of Variations and Euler's Elastica</b>	<b>24</b>
3.1 Preliminaries . . . . .	24
3.2 Calculus of variations . . . . .	25
3.3 Calculus of variations with constraints . . . . .	26
3.4 Euler's Elastica . . . . .	30
Linearization of Euler's Elastica Equation: . . . . .	33
3.5 Numerical methods and examples . . . . .	36
3.6 Analytical methods to solve Euler's Elastica (elliptic integrals) . . . . .	38
<b>4 Nonlinear Beam Theory</b>	<b>40</b>
4.1 Strain-displacement relations for a nonlinear beam . . . . .	40
4.2 Simplifications of the general theory . . . . .	43
4.3 First-order constitutive relation for linear elastic behavior . . . . .	46
4.4 Equations of equilibrium from variational methods . . . . .	46
4.5 Small strain, moderate rotation for circular rings . . . . .	48





# 1 Beams: Traction, Bending, Torsion and Buckling

**Beams** are elongated structural elements that are submitted to one (or more) internal load(s), offering resistance to bending (and/or torsion, and/or shear) due to applied forces (and/or moments).

It is important to note that if there is a well-established convention for the directions of internal loads, as shown in Fig. 1.1, that is not the case for the choice of the coordinate system. That is, one can choose to employ either a right-handed or a left-handed coordinate system, at will. For example, [Stephen Timoshenko](#) (1878-1972), one of the 'fathers' of modern engineering mechanics, used left-handed coordinate systems throughout his works. Even though this may not be standard in physics or mathematics, left-handed systems are, thus, widely used in the field of structural mechanics.

- 1.1 Beam bending . . . . . 1
- 1.2 Torsion of rods and shafts . . 5
- 1.3 Summary of stretching, bending and torsion of rods . . . . . 7
- 1.4 Castiglino's theorem . . . . . 8
- 1.5 Buckling of beams . . . . . 9

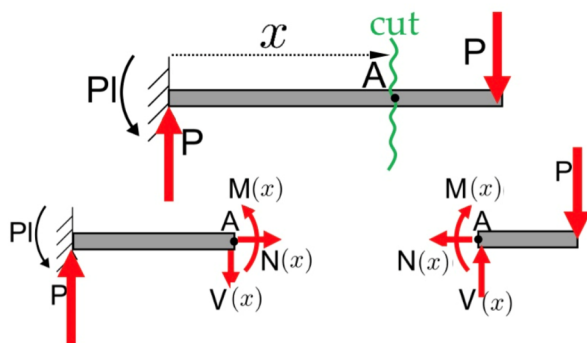


**Figure 1.1:** The internal loads are the axial load  $N(x)$ , the shear force  $V(x)$  and the internal moment  $M(x)$ .

## 1.1 Beam bending

### Moment-curvature relation

We start by reviewing how the moment  $M$  applied to a beam is related to ensuing deformation in the case of pure bending (see Fig. 1.2); *i.e.*,

when the only external loads are moments of same amplitude applied at both extremities of the beam. The procedure that we will follow to arrive at the moment-curvature relation involves the following steps: (i) make a kinematic approximation that allows us to assume simple motion, (ii) calculate the stress field given the said simple motion, and, finally, (iii) integrate the stress field to obtain expressions for both forces and moments.

**Step (i): Kinematics**

For simplicity, and without loss of generality, we will consider the cross-section of a rectangular beam under pure bending. Importantly, we assume that perpendiculars to the centerline of the beam remain perpendicular (see Fig. 1.3), and that the centerline does not stretch. Even though these assumptions are, of course, not exact, they are a good approximation if the beam is slender. For a beam to be considered as slender, we require that the characteristic length scales associated with the cross section (*e.g.*, width and thickness, or the radius if the cross-section of the beam is circular) are much smaller than the length of the beam:  $h, w, r \ll \ell$ .

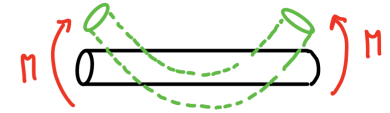
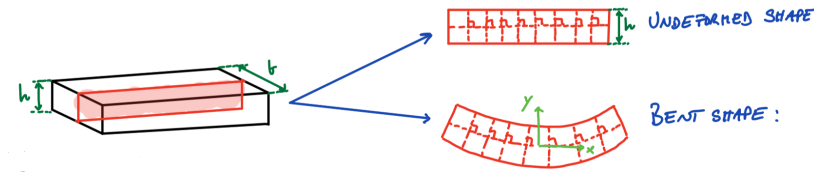


Figure 1.2: Beam under pure bending

Figure 1.3: Cross-section of a rectangular beam

From geometry (see Fig. 1.4), we get that

$$\frac{l}{L} = \frac{\Delta\theta(r - y)}{\Delta\theta r} = 1 - \frac{y}{r}. \tag{1.1}$$

Therefore, the axial strain in  $x$ -direction is

$$\epsilon_{xx} = \frac{l - L}{L} = \frac{L(1 - \frac{y}{r}) - L}{L} = -\frac{y}{r}. \tag{1.2}$$

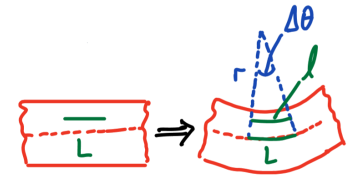


Figure 1.4: Zoom in;  $r$  is radius of curvature

**Step (ii): Stress Field**

Given the motion assumed above, and since the beam is thin,  $\sigma_{xy}$  and  $\sigma_{yy}$  remain small through thickness, hence,

$$\sigma_{xy}, \sigma_{yy} \ll \sigma_{xx}. \tag{1.3}$$

The above statement in Eq. (1.3) means that each fiber in the beam is in a state of pure tension (no shear), such that,

$$\sigma_{xx} = E\epsilon_{xx} = -\frac{y}{r}E. \tag{1.4}$$

In words, Eq. (1.4) reflects the fact that stress is compressive above the centerline, and tensile below (for the configuration shown in Fig. 1.4).

**Step (iii): Forces and Moments**

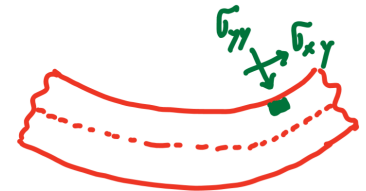


Figure 1.5: Nothing touching on both top and bottom surfaces, hence  $\sigma_{yy}(y + \pm h/2) = 0$  and  $\sigma_{xy}(y + \pm h/2) = 0$

The total force at the extremities of the beam can be obtained by integrating the tensile stress over the cross sections, yielding

$$F_x = \int_{\text{cross section}} \sigma_{xx} dA = \int_0^b \int_{-h/2}^{h/2} -E \frac{y}{r} dy dz = 0. \quad (1.5)$$

The above null is to be expected since the configuration is symmetric with respect to the centerline.

For the total moment, we have

$$\begin{aligned} M &= \int \mathbf{r} \times \mathbf{F} = \int_A \langle 0, y \rangle \times \langle 1, 0 \rangle \sigma_{xx} dA = \hat{\mathbf{z}} \int_A y E \frac{y}{r} dA \\ &= \hat{\mathbf{z}} \int_A E y^2 \frac{1}{r} dx dy = \hat{\mathbf{z}} \frac{E}{r} \int_A y^2 dA. \end{aligned} \quad (1.6)$$

Finally, we obtain the *moment-curvature relation*

$$M = \frac{EI}{r} = EI\kappa, \quad (1.7)$$

$\kappa = 1/r$  is the curvature and  $EI$  is the bending stiffness of the beam.

where

$$I = \int_A y^2 dA \quad (1.8)$$

is the moment of inertia (sometimes also referred to as the second moment of area).

Rectangular cross section:  $I = bh^3/12$   
Circular cross section:  $I = \pi R^4/4$

We now want to be able to state what the actual deflection of the beam  $u_y(x)$ , given an applied moment  $M$ .

### Small-deflection approximation

Let us assume that:

- ▶ Points on the deformed centerline remain close to their original position (*i.e.*, the deflection of the beam is small)".
- ▶ Before and after the deformation, the centerline has nearly the same length (inextensibility assumption)

Often, it is common in structural mechanics to use " $w(x)$ " instead of " $u_y(x)$ " for deflection, which is therefore the notation that we will also use hereon.

We recall that curvature is defined as:

$$\kappa = \frac{w''}{(1 + w'^2)^{3/2}} \approx w''(x), \quad (1.9)$$

which when  $w' \ll 1$  reduces to

$$\kappa \approx w''(x), \quad (1.10)$$

In the limit of small deflection, the moment-curvature relation derived above becomes

$$M = EI \frac{d^2 w}{dx^2}, \quad (1.11)$$

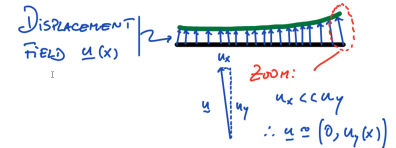


**Figure 1.6:** The displacement along the  $x$  direction can be neglected for small deflections;  $\mathbf{u} \approx (0, u_y(x))$

and the corresponding axial stress is

$$\sigma_{xx} = -\kappa E y = -\frac{M y}{I}. \quad (1.12)$$

### Elastic energy stored due to bending of an originally straight beam

Given the assumptions that we have taken thus far, the elastic energy of a beam of length  $L$  can be computed as

$$\begin{aligned} \mathcal{E} &= \frac{1}{2} \int_L dx \int_A dA \sigma_{ij} \epsilon_{ij} = \frac{1}{2} \int_L dx \int_A dA \sigma_{xx} \epsilon_{xx} \\ &= \frac{E}{2r^2} \int_L dx \int_A dA y^2 = \frac{1}{2} \int_L \frac{E dx}{r^2} \int_A dA y^2 \\ &= \int_L \frac{EI}{2r^2} dx. \end{aligned} \quad (1.13)$$

Later in this course, we will also use the notation  $\mathcal{U}_b$  to express the bending energy (in contrast to the stretching energy  $\mathcal{U}_s$ ).

### Beam equation

Considering a distributed load  $q(x)$  along the beam, invoking the total sum of forces and moments yields

$$\begin{aligned} \sum F_y = 0 &\Rightarrow \frac{dV(x)}{dx} = -q(x), \\ \sum M_O = 0 &\Rightarrow \frac{dM(x)}{dx} = V(x). \end{aligned} \quad (1.14)$$

Hence,

$$\frac{d^2 M}{dx^2} = -q(x). \quad (1.15)$$

Recalling that  $M = EI w''(x)$ , we finally get that

$$q(x) = -\frac{d^2}{dx^2} \left( EI \frac{d^2 w}{dx^2} \right). \quad (1.16)$$

The above fourth-order ordinary differential equation can be solved given appropriate boundary conditions.

### Example: Atomic force microscope

An atomic force microscope (AFM) can be used to detect individual atoms. The key mechanical element of an AFM is a silicon cantilever beam, to the end of which an atomically sharp tip is attached. When the tip is close enough to the surface that is being probed, there is an attractive force,  $F_a$ , between the atom at the very end of the tip and the atom in the surface below it. The attractive force induces a state of bending in the beam, whose deflection can be measured through optical means.



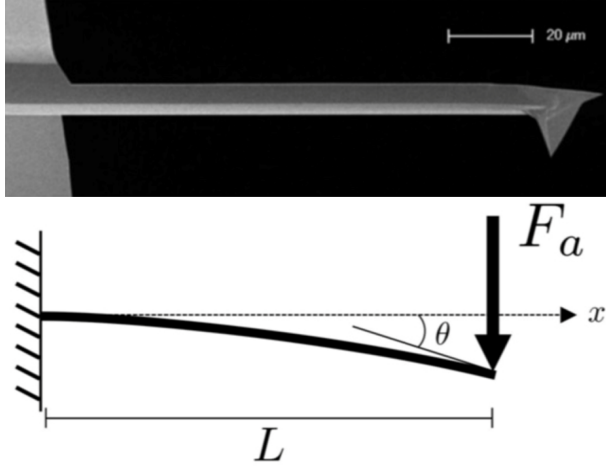


**Figure 1.7:** Atomic force microscope (top). Free-body diagram of the considered AFM structure (bottom).

By imposing equilibrium of moments at the clamp, we can readily get that

$$M(x) = F_a(x - L). \quad (1.17)$$

Since we are considering small displacements, integrating the beam equation twice gives us

$$EIw(x) = F_a \left( \frac{x^3}{6} - \frac{Lx^2}{2} \right) + C_1x + C_2, \quad (1.18)$$

where  $C_1$  and  $C_2$  are constants of integration that need to be determined from the boundary conditions. At the clamp, we have zero slope and zero deflection, which immediately leads to

$$C_1 = C_2 = 0. \quad (1.19)$$

Thus, at the free-end ( $x = L$ ), the displacement is

$$w(L) = -\frac{F_a L^3}{3EI}. \quad (1.20)$$

After rearranging Eq. (1.20) as

$$F_a = -\frac{3EI}{L^3} w(L), \quad (1.21)$$

we recognize that the effective spring constant of the cantilever is

$$k = \frac{3EI}{L^3}. \quad (1.22)$$

## 1.2 Torsion of rods and shafts

Let us start by inverting the stress-strain relation of 3D isotropic linear elasticity to express the strain as a function of the stress,

$$\epsilon = \frac{1}{E} [\sigma(1 + \nu) - \nu(\text{tr } \sigma)\mathbf{I}], \quad (1.23)$$

which for the shear strain component of  $\epsilon$  yields

$$\epsilon_{xy} = \frac{1 + \nu}{E} \sigma_{xy} \tag{1.24}$$

Recalling that the shear modulus can be expressed as a function of the Young's modulus,  $E$ , and the Poisson's ratio,  $\nu$ ,

$$G = \frac{E}{2(1 + \nu)}, \tag{1.25}$$

we finally get that

$$\sigma_{xy} = 2G\epsilon_{xy} = G\gamma_{xy}, \tag{1.26}$$

where  $\gamma_{xy} = 2\epsilon_{xy}$  is typically referred to as the engineering shear strain.

Let us now apply opposing torques to ends of rod, thus putting it under a state of torsion.

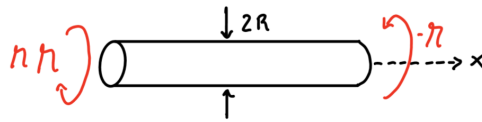


Figure 1.8: Rod under torsion

To be accurate with semantics, let us remark that 'twist' is a statement on kinematics, whereas 'torsion' is the mechanical response of a body subject to the application of torques at its extremities.

**Simplifying assumptions**

We further assume that:

- ▶ During torsion, there are no displacements in the axial direction, hence  $\epsilon_{xx} = 0$ ,
- ▶ Each cross-section moves only by rotation on its plane; *i.e.*, there is only relative rotation between two cross-sections,
- ▶ In the cylindrical basis:  $\epsilon_{rr} = 0, \epsilon_{\theta\theta} = 0, \epsilon_{r\theta} = 0$

Consequently, under above assumptions for small deformations, in-plane angles do not change and in-plane lines do not stretch. A twisted column is thus put under state of simple shear.

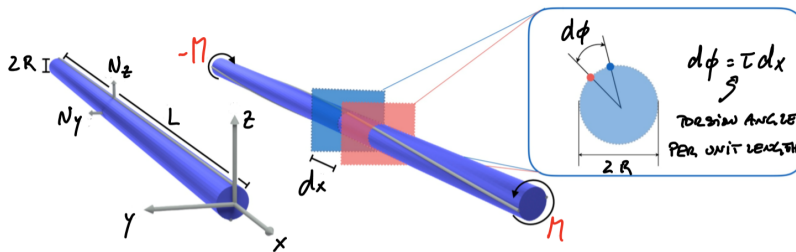


Figure 1.9: Therefore, if  $\phi(x) \neq \text{constant}$ , the shaft is twisted.

From geometry (see Fig. 1.9 and Fig. 1.10), we get that

$$\gamma_{x\theta} = \tan^{-1} \left( \frac{r d\phi}{dx} \right) \approx r \frac{d\phi}{dx} = r\tau, \tag{1.27}$$

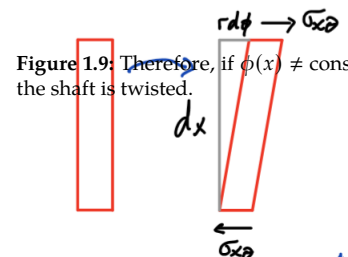


Figure 1.10:  $\gamma_{x\theta}$  increases with r

where  $\tau = \frac{d\phi}{dx}$  is defined as the *twist per unit length*.

Now, invoking linear elasticity, we can state that

$$\sigma_{x\theta} = G\gamma_{x\theta} = Gr \frac{d\phi}{dx}. \quad (1.28)$$

The internal torque can be computed by integrating the shear stress over the cross section,

$$M(x) = \int_A r\sigma_{x\theta} dA = \int_A rGr \frac{d\phi(x)}{dx} dA = G \frac{d\phi(x)}{dx} \int_A r^2 dA, \quad (1.29)$$

where we recognize  $J \equiv \int_A r^2 dA$  as the *polar moment of inertia*. Hence,

$$M(x) = GJ \frac{d\phi(x)}{dx} = GJ\tau, \quad (1.30)$$

which is a relation relating the twist by unit length,  $\tau$ , to the torsional stiffness,  $GJ$ . It is interesting to compare the result in Eq. (1.30) with the moment-curvature relation for pure bending in Eq. (1.11), reproduced here again for convenience:

$$M(x) = EI \frac{d^2w(x)}{dx^2} = EI\kappa$$

We note that, for the case of pure bending, the moment depends linearly on curvature (with the bending stiffness,  $EI$ , as the constant of proportionality), whereas for pure torsion, the moment depends linearly on the twist per unit length (with the torsional stiffness,  $GJ$ , as the constant of proportionality).

### Elastic energy stored in pure torsion of rod

For small deformations, the total energy in rod of length  $L$ , cross-section  $A$  and volume  $V$  is

$$\begin{aligned} \mathcal{E}_t &= \frac{1}{2} \int_V \sigma_{x\theta} \epsilon_{\theta x} dV = \frac{1}{2} \int G\tau^2 r^2 dV \\ &= \frac{1}{2} \int G\tau^2 dx \int_A r^2 dA. \end{aligned} \quad (1.31)$$

Substituting what we got from above, we finally get that

$$\mathcal{E}_t = \frac{1}{2} \int_L GJ\tau^2 dx = \frac{1}{2} \int_L \frac{M^2}{GJ} dx. \quad (1.32)$$

## 1.3 Summary of stretching, bending and torsion of rods

The following table summarizes all of the important results that we have obtained above, for three fundamental modes of deformation in a beam:

Solid circular cross section:  $J = \frac{\pi R^4}{2}$   
Thin tube (radius  $R$ , thickness  $t$ ):  $J = 2\pi R^3 t$

axial stretching, pure bending and pure torsion.

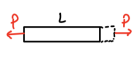


	$EA$ AXIAL STIFFNESS	$F = EA \frac{du}{dx}$	$\mathcal{E}_s = \frac{1}{2} \int_L EA \epsilon^2 dx = \frac{1}{2} \int_L \frac{P^2}{EA} dx$
	$EI$ BENDING STIFFNESS	$\eta = EI \frac{d^2\omega}{dx^2}$	$\mathcal{E}_b = \frac{1}{2} \int_L \frac{EI}{R^2} dx = \frac{1}{2} \int_L \frac{M^2}{EI} dx$
	$GJ$ TORSIONAL STIFFNESS	$\eta = GJ \frac{d\phi}{dx}$	$\mathcal{E}_t = \frac{1}{2} \int_L GJ \tau^2 dx = \frac{1}{2} \int_L \frac{M^2}{GJ} dx$

Table 1.1: Stretching vs. bending vs. torsion of rods

### 1.4 Castiglino’s theorem

**Castiglino’s Theorem**

If the total elastic energy in a body,  $\mathcal{E}$ , is expressed in terms of the external loads, then, the in-line deflection  $\delta_i$  of the point of application of a particular load  $P_i$  is given by:

$$\delta_i = \frac{\partial \mathcal{E}}{\partial P_i}. \tag{1.33}$$

**Example 1.4.1 Stiffness of a helical coil spring:**

A load  $P$  is applied to the extremity of a helical coil spring, as presented in the schematic diagrams of Fig. 1.11. Equilibrium of forces yields that the shear force in the wire is  $P$ , and, thus, the corresponding moment is  $RP$ . To good approximation, we assume that each loop of wire in the helical structure is in a state of simple torsion. The total strain energy for the whole spring is thus

$$\begin{aligned} \mathcal{E} &= \int_L \frac{M^2}{2GJ} dz = \int_L \frac{P^2 R^2}{2GJ} dz = \frac{P^2 R^2}{2GJ} 2\pi RN \\ &= \frac{\pi NP^2 R^3}{GJ}. \end{aligned} \tag{1.34}$$

Invoking Castiglino’s theorem gives

$$\delta = \frac{\partial \mathcal{E}}{\partial P} \Rightarrow \delta = \frac{PR^3}{GJ} 2\pi N = \frac{8PR^3 N}{Gr^4}, \tag{1.35}$$

which can be rearranged to obtain an expression for the spring constant:

$$k = \frac{P}{\delta} = \frac{Gr^4}{4NR^3}. \tag{1.36}$$

For example,  $k$  doubles when the radius of each look in the helical wire increases by 19%.

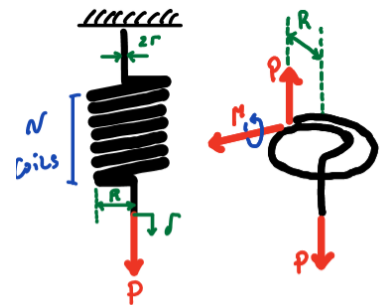
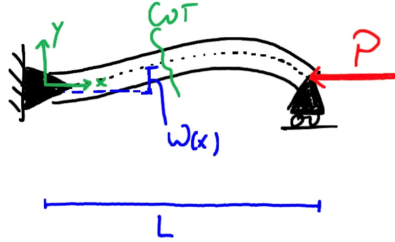


Figure 1.11: Coil spring; length of each coil is approximately  $2\pi R$ .

## 1.5 Buckling of beams

Buckling is an instability of elastic structures under compression that induces bending. In this section, we will expand linearized beam theory presented above to admit a compressive internal load, albeit assuming no compressive deformation; *i.e.*, all motion will be just due to bending.

As a first illustrative example, we focus on the specific case of a beam pin-pin boundary conditions (see Fig. 1.12), such no moments are generated at the boundaries, and the vertical displacements are constrained there.



**Figure 1.12:** Buckling of a beam with pin-pin boundary conditions due to the application of an axial load,  $P$ .

We take an imaginary cut and use the method of sections to compute the internal loads in the beam. Given that deformations are small, it is reasonable to assume that

$$\begin{aligned} V &\approx -V(x)\hat{y} \\ N &\approx N(x)\hat{x}, \end{aligned} \quad (1.37)$$

meaning that the internal normal load  $N$  is nearly horizontal and the internal shear load  $V$  remains nearly vertical (perpendicularly to the centerline), following the coordinate system defined in Fig. 1.12. A graphical representation of the approximating assumption expressed in Eq. (1.37) is shown in Fig. 1.14.

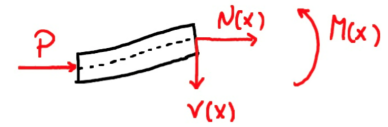


**Figure 1.13:** Small deformation approximation

The balance of forces and moment of the system at hand yields:

$$\begin{aligned} \sum F_x = 0: \quad P + N &= 0 \Rightarrow N(x) = -P \\ \sum F_y = 0: \quad &\Rightarrow V(x) = 0 \\ \sum M_O = 0: \quad M - w(x)N - xV(x) &= 0 \Rightarrow M(x) = -Pw(x), \end{aligned} \quad (1.38)$$

and the moment-curvature relation reads

$$EI \frac{d^2w}{dx^2} = M = -Pw \Rightarrow EI \frac{d^2w}{dx^2} + Pw = 0, \quad (1.39)$$

Eq. (1.39) is an ordinary differential equation (O.D.E.) for the deflection  $w(x)$  whose general solution is

$$w(x) = C_1 \sin\left(\sqrt{\frac{P}{EI}}x\right) + C_2 \cos\left(\sqrt{\frac{P}{EI}}x\right). \quad (1.40)$$

where  $C_1$  and  $C_2$  are constants that be determined from the appropriate boundary conditions. Since there is no deflection a either extremity of

the beam,  $w(0) = w(L) = 0$ , we readily find that

$$C_2 = 0 \quad \text{and} \quad C_1 \sin\left(\sqrt{\frac{P}{EI}}L\right) = 0. \quad (1.41)$$

The second condition in Eq. (1.41) is satisfied if  $C_1 = 0$ , such that  $w(x) = 0$ , which corresponds to the trivial (straight) solution. Alternatively, the second condition in Eq. (1.41) can also be satisfied when  $\sin\left(\sqrt{\frac{P}{EI}}L\right) = 0$ , which is the buckled solution of interest. For this buckled solution, we it is required that

$$\sqrt{\frac{P^{*(n)}}{EI}}L = n\pi \quad \Rightarrow \quad P^{*(n)} = \frac{n^2\pi^2EI}{L^2} \quad (1.42)$$

where  $n$  is an integer, and  $P^{*(n)}$  is the critical buckling load corresponding to the  $n$ -th mode. The lowest value for critical buckling load occurs when  $n = 1$ ,

$$P_{cr} = P^{*(1)} = \frac{\pi^2EI}{L^2}, \quad (1.43)$$

which is traditionally referred to as the classic *Euler buckling load* of a beam.

For loads lower than the critical buckling load  $P < P_{cr}$ , the beam maintains the straight solution (see Fig. 1.14, top). Buckling occurs when  $P \geq P_{cr}$  and the beam assumes a non-straight configuration (see Fig. 1.14, bottom). The linear analysis performed above does now allow us to determine neither the amplitude of the buckled solution,  $C_1$ , nor the shape of the beam in the post-buckling regime ( $P > P_{cr}$ ). We will learn how to do this in subsequent lectures, later in this course.

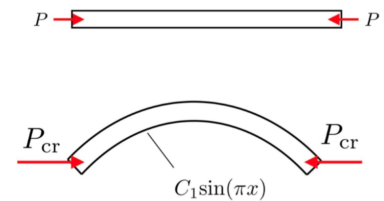


Figure 1.14: Lowest load when  $n = 1$ .

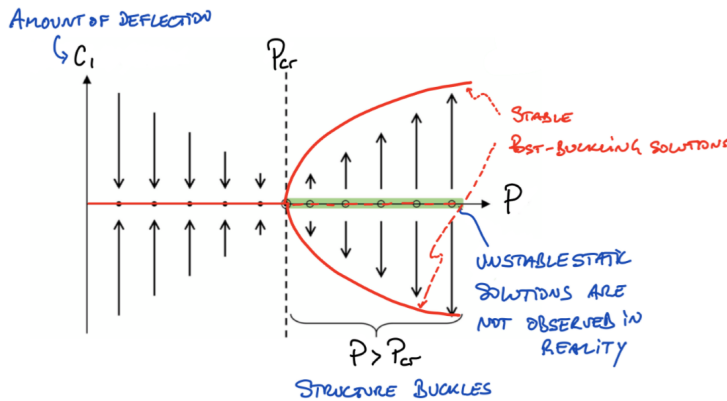


Figure 1.15: Bifurcation diagram

Through a nonlinear analysis (beyond the scope of these review notes), it would have been possible to compute a bifurcation diagram to further expand on the analysis performed above (see Fig. 1.15). Below the critical buckling load  $P < P_{cr}$ , the extent of deflection, as quantified through the amplitude  $C_1$ , is trivially zero and the straight solution is stable. Above  $P \geq P_{cr}$  the straight solution becomes unstable and, upon an infinitesimal perturbation, the beam exhibits its stable post-buckling solution, whose amplitude scales as the square root of the applied load,  $\sqrt{P}$ . It can be shown that when  $P > P_{cr}$ , the  $C_1 = 0$  solution is unstable, and therefore is never observed in reality.

A more formal analysis of this problem will be addressed in detail when we introduce the geometrically nonlinear theory of inextensible beams, also known as *Euler's Elastica*, in Lecture 3.

**Higher order buckling loads of an axially compressed beam**

It is possible to reach higher order buckling modes by preventing the lower order buckling modes from occurring. For example, we can modify the system analyzed above to inhibit the  $n = 1$  solution by constraining the beam at its mid-span using a pinned connection as shown Fig. 1.16. The corresponding second-order ( $n = 2$ ) buckling load is

$$P^{*(n=2)} = (2\pi)^2 \frac{EI}{L^2}, \tag{1.44}$$

and the associated displacement function is

$$w_2(x) = C_1 \sin \left( \sqrt{\frac{P^{*(n=2)}}{EI}} x \right) = C_1 \sin \left( \frac{2\pi x}{L} \right), \tag{1.45}$$

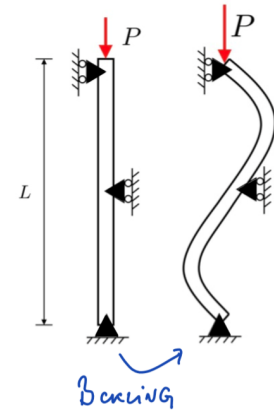


Figure 1.16:  $n = 2$  case.

which is a full wavelength compared to the the half-wavelength for the  $n = 1$  case. Similarly, to excite the  $n = 3$  solution, we need to prevent both the  $n = 1$  and the  $n = 2$  solutions. More generally, to excite the  $N$ -th solution, we need to prevent all  $1 \leq n \leq N - 1$  solutions.

Above, we focused our discussion exclusively on axially loaded beams pinned at both extremities (*i.e.*, the pin-pin case). If the ends are constrained by supports other than pins, following a similar procedure but with different boundary conditions would give

$$P_{cr} = \frac{\pi^2 EI}{(KL)^2}, \tag{1.46}$$

where  $K$  is the effective length factor, which depends on the type of end constraints. The examples in Fig. 1.17 represent a few typical cases:

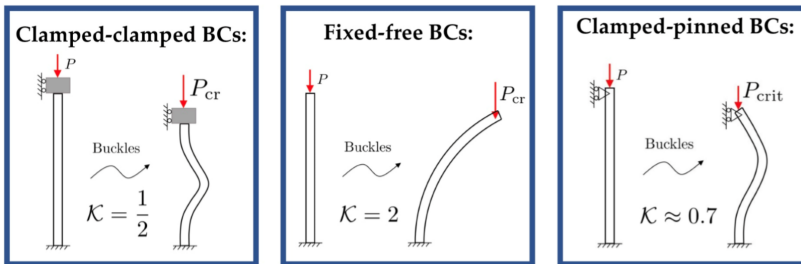


Figure 1.17: Example of buckled beams with clamped-clamped (left), fixed-free (middle), and clamped-pinned (right) boundary conditions, along with the corresponding value of the effective length factor,  $K$ , which modifies the critical buckling load in Eq. (1.46).

$K = 1/2$ ,  $K = 2$ , and  $K \approx 0.7$ , respectively, for the cases of clamped-clamped, fixed-free, and clamped-pinned boundary conditions.



## 2 Dimensional Analysis and Scalings

### 2.1 Introduction

Our goal in this chapter is to develop a methodology to solve physical problems, even if approximately, by identify relationships between physical quantities and the relevant parameters through a procedure that is often referred to as *Dimensional Analysis*. This method of *Dimensional analysis* is based on the premises that:

1. Any physical law must be expressible independently of system of units.
2. The description and definition of a physical problem must respect consistency between dimensions.

The two premises above have the important consequence that one is able to *guess* (estimate) approximate solutions by reasoning with the relevant dimensions of a problem. Moreover, scientifically interesting results are always expressible in terms of dimensionless quantities or groups. The technique of dimensional analysis requires a mix of sharp physical intuition and rigour, which we will formalize using the Buckingham- $\Pi$  theorem.

### 2.2 Base dimensions and units

Fundamental physical dimensions are quantified by units, such as the International System of Units, which is often abbreviated as *SI* (from the French: *Système International (d'unités)*). For example, we measure length is *meter* (m), mass in *kilogram* (Kg), time in *seconds* (s), and temperature in *Kelvin* (K).<sup>1</sup> Let us assume that there exists a system of  $q$  fundamental physical dimensions, from which all other dimensions of physical quantities can be derived. Typically, in mechanics,  $q = 3$  : ( $L$  for length,  $M$  for mass, and  $T$  for time). Sometimes, temperature,  $\Theta$ , must also be considered, such that  $q = 4$ . One typically refers to the units of a

2.1 Introduction . . . . .	12
2.2 Base dimensions and units . . . . .	12
2.3 Buckingham- $\Pi$ Theorem . . . . .	15
2.4 Summary of the recipe to solve a problem using dimensional analysis . . . . .	16
2.5 Extended dimensional analysis . . . . .	17
2.6 Physical similarity . . . . .	19
2.7 Scalings . . . . .	20

<sup>1</sup>: Note that when typesetting units, they are typically not set in *italic*, for example:

$$M = 74 \text{ Kg}$$



physical quantity by using the square brackets  $[\cdot]$ . For a general quantity, whose units are we have

$$[q] = L^a M^b T^c, \quad (2.1)$$

where the exponents  $a$ ,  $b$ , and  $c$  can be any real number.

**Example 2.2.1 Dimensions and units:**

Thickness:	$[h] = L$
Volume:	$[V] = L^3$
Gravitational acceleration:	$[g] = LT^{-2}$
Force:	$[F] = MLT^{-2}$
Strength:	$[\sigma_0] = [F]L^{-2} = L^{-1}MT^{-2}$

Galileo Galilei (1564-1642) was the first to recognize that similar objects, no matter their shape, can be related through scaling laws. In his canonical book *Two New Sciences*<sup>2</sup> he asked the following questions:

- ▶ Why is an elephant is different than a giant mouse?
- ▶ Why are there ultimate limits to the size of animals, plants, and structures?
- ▶ Why would giant humans, if they existed, face structural problems?

2: In Italian: *Discorsi e dimostrazioni matematiche intorno a due nuove scienze attinenti la meccanica e i movimenti locali* (1638).

**Example 2.2.2 The mechanics of giants:** Motivated by Galileo's reasoning, we seek to determine the maximum load capacity that a giant, if they existed, could take without collapsing under their own weight. This problem translates into determining the conditions for which the weight of the giant is smaller than a limit force depending on its characteristics, which we can express mathematically as

$$mg \leq F_{\text{lim}} = f(h, g, \rho, V, \sigma_0), \quad (2.2)$$

where  $F_{\text{lim}}$  is the maximum load bearing capacity,  $h$  is the height of the giant,  $\rho$  its density,  $V$  its volume,  $\sigma_0$  the maximal tensile stress that its bones can support, and  $g$  is the gravitational acceleration. The set of variables  $(h, g, \rho, V, \sigma_0)$  forms a *complete* set of *independent* variables. By *complete*, it is meant that no other quantities affect  $F_{\text{lim}}$ . By *independent*, it is meant that the value of these variables can be set arbitrarily without influencing one another.

Eq. (2.2) is relevant only if it is dimensionally homogeneous, such that,

$$[F_{\text{lim}}] = [f] = LMT^{-2}. \quad (2.3)$$

Through a rationale that will be further formalized (and justified) below once we introduce the Buckingham- $\Pi$  theorem, we need the dimensions of  $f$  to be expressed as a function of 3 of the 4 variables  $(h, g, \rho, \sigma_0)$  or  $(V, g, \rho, \sigma_0)$  since  $h$  and  $V$  are dimensionally *dependent*. Below, in Eq. (2.6), we will arbitrarily pick the set  $(h, g, \text{ and } \sigma_0)$  as the bases to express the unigs of  $F_{\text{lim}}$ ,  $\rho$ , and  $V$ . Also, for simplicity, and to a first approximation, we are considering that the shape of the giant is a sphere.

In summary, the dimensions of the various quantities involved in the problem are as follows:

$$\begin{aligned}
 [F_{lim}] &= [f] = LMT^{-2} \\
 [h] &= L \\
 [V] &= L^3 \\
 [g] &= LT^{-2} \\
 [\rho] &= L^{-3}M \\
 [\sigma_0] &= [F_{lim}]L^{-2} = L^{-1}MT^{-2}
 \end{aligned} \tag{2.4}$$

As an alternative way to express the results in Eqs. (2.4) we can use the following matrix form:

$$\begin{array}{c|cccccc}
 & [F_{lim}] & [h] & [V] & [g] & [\rho] & [\sigma_0] \\
 \hline
 L & 1 & 1 & 3 & 1 & -3 & -1 \\
 M & 1 & 0 & 0 & 0 & 1 & 1 \\
 T & -2 & 0 & 0 & -2 & 0 & -2
 \end{array} \tag{2.5}$$

Note that the second and third columns correspond to the dimensionally *dependant* quantities, whereas the quantities in the fourth, fifth and sixth columns correspond to the dimensionally *independent* quantities. The usefulness of the matrix representation in Eq. (2.4.1) will become more apparent once we introduce the Buckingham- $\Pi$  theorem (Section 2.3).

Recalling that dimensions of a general quantity can be expressed as  $[q] = L^a M^b T^c$ , we now write

$$\begin{aligned}
 [F_{lim}] &= [h]^{a_1} [g]^{a_2} [\sigma_0]^{a_3} \\
 [\rho] &= [h]^{b_1} [g]^{b_2} [\sigma_0]^{b_3} \\
 [V] &= [h]^{c_1} [g]^{c_2} [\sigma_0]^{c_3},
 \end{aligned} \tag{2.6}$$

where  $a_i$ ,  $b_i$  and  $c_i$  are numerical exponents (for  $i = \{1, 2, 3\}$ ). By inspection of  $[V]$ , we can readily see that  $c_1 = 3$  and  $c_2 = c_3 = 0$ . For the density,  $\rho$  (with  $[\rho] = L^{-3}M$ ) we have to perform a more careful analysis. The consistency of the units of  $\rho$  can be expressed using the exponents  $b_1$ ,  $b_2$ , and  $b_3$  of the dimensions of  $[h]$ ,  $[g]$ , and  $[\sigma_0]$ , respectively, in matrix form as

$$\begin{pmatrix} -3 \\ 1 \\ 0 \end{pmatrix} = \begin{bmatrix} 1 & 1 & -1 \\ 0 & 0 & 1 \\ 0 & -2 & -2 \end{bmatrix} \begin{pmatrix} b_1 \\ b_2 \\ b_3 \end{pmatrix}, \tag{2.7}$$

where the vector in the left hand side of the equation lists the exponents of  $L$ ,  $M$ , and  $T$  that are relevant for  $\rho$ , and in the  $3 \times 3$  matrix of the right-hand-side of the equation, the 1st, 2nd, and 3rd rows are, respectively, the units  $L$ ,  $M$ , and  $T$ , and the 1st, 2nd, and 3rd columns are the exponents associated with  $[h]$ ,  $[g]$ , and  $\sigma_0$ . Eq. (2.7) can be solved to obtain  $b_1 = b_2 = -1$  and  $b_3 = 1$ . Hence,

$$[\rho] = \frac{[\sigma_0]}{[h][g]} \tag{2.8}$$

We can follow a similar procedure for both  $F_{lim}$  and  $V$  to find:

$$\begin{aligned} [F_{lim}] &= [h]^2[\sigma_0] \\ [V] &= [h]^3. \end{aligned} \quad (2.9)$$

We can thus identify 3 dimensionless groups,

$$\begin{aligned} \Pi_0 &= \frac{F_{lim}}{h^2\sigma_0}, \\ \Pi_1 &= \frac{hg\rho}{\sigma_0}, \\ \Pi_2 &= \frac{V}{h^3}, \end{aligned} \quad (2.10)$$

even if we will show that only two of these are independent.

Recall that we formulated our problem as  $mg \leq F_{lim} = f(H, g, \rho, V, \sigma_0)$ . Introducing Eqs. (2.10) into Eq. (2.2), we get that

$$\begin{aligned} \Pi_0 &= \frac{1}{h^2\sigma_0} f(h, g, \rho = \frac{\Pi_1\sigma_0}{hg}, V = \Pi_2h^3, \sigma_0) \\ \Rightarrow \Pi_0 &= F(h, g, \Pi_1, \Pi_2, \sigma_0). \end{aligned} \quad (2.11)$$

Since  $\Pi_0$  is dimensionless,  $F$  must also be dimensionless, which can be satisfied *if and only if*  $F$  is independent of  $(h, g, \sigma_0)$ ; *i.e.*,

$$\Pi_0 = \frac{F_{lim}}{h^2\sigma_0} = F(\Pi_1 = \frac{hg\rho}{\sigma_0}, \Pi_2 = \frac{V}{h^3}). \quad (2.12)$$

In summary, based on dimensional analysis, we reduced a dimensional problem parameterized by 5 dimensional parameters to a dimensionless problem that depends only on 2 dimensionless groups (parameters). The formalization of the procedure that we have just followed will be presented next, in Section 2.3.

## 2.3 Buckingham- $\Pi$ Theorem

Consider a relation between  $N + 1$  dimensional physical quantities:  $q_0 = f(q_1, q_2, \dots, q_N)$ . Let  $k$  be the number of dimensionally independent variables  $q_1, q_2, \dots, q_k$ , which are a subset of  $q_1, q_2, \dots, q_N$ . The initial physical relation can be reduced to a dimensionless relation between  $N - k + 1$  dimensionless groups  $\Pi_0, \Pi_1, \dots, \Pi_{N-k}$ :

$$\Pi_0 = F(\Pi_1, \dots, \Pi_{N-k}), \quad (2.13)$$

defined by

$$\Pi_i = \frac{q_i}{q_1^{a_1^i} q_2^{a_2^i} \dots q_k^{a_k^i}}, \quad i \in \{0, N - k\}, \quad (2.14)$$

Where the exponent  $a_1^i, \dots, a_k^i$  are determined from the dimensionless functions  $[q_i] = [q_1]^{a_1^i} [q_2]^{a_2^i} \dots [q_k]^{a_k^i}$ .

## 2.4 Summary of the recipe to solve a problem using dimensional analysis

1. **Formulate the problem:** Write a relation between a dependant variable and a complete set of  $N$  independent variables.
2. **Determine the dimensionally independent variables:** Build the exponent matrix of the dimensions of the  $N + 1$  parameters and determine the rank  $k$  of the matrix.
3. **Construct  $N - k + 1$  dimensional groups:** Choose  $k$  dimensionally independent variables and express the remaining  $N - k + 1$  variables, so that expressions are dimensionless.
4. **Explore the dimensionless relations.**

The number of dimensionally independent variables  $k$  corresponds to the *rank* of the exponent matrix of dimensions.

The rank of a matrix is the maximal number of linear independent rows or columns. The most convenient way to determine this is to manually identify the dimensions of the largest non-singular sub-square matrix  $[A_{kk}]$  of  $[A_{q(N+1)}]$  *i.e.*, with determinant  $\det[A_{kk}] \neq 0$ , where  $q$  is the number of base dimensions.

**Example 2.4.1 Rank of a matrix** In the Example 2.2.2, above, we had written the corresponding exponent matrix in Eq. (2.4.1), rewritten here for convenient, as

$$\begin{array}{c|cccccc} & [F_{\text{lim}}] & [h] & [V] & [g] & [\rho] & [\sigma_0] \\ \hline L & 1 & 1 & 3 & 1 & -3 & -1 \\ M & 1 & 0 & 0 & 0 & 1 & 1 \\ T & -2 & 0 & 0 & -2 & 0 & -2 \end{array}$$

The rank of this matrix,  $k$  is at most 3 (largest possible sub-square matrix) but we first need to check which sub-square matrix is non-singular *i.e.*,  $\det[\cdot] \neq 0$ .

$$\det \begin{vmatrix} 1 & 3 & 1 \\ 0 & 0 & 0 \\ 0 & 0 & -2 \end{vmatrix} = 0 \quad (2.15)$$

but

$$\det \begin{vmatrix} 1 & -3 & -1 \\ 0 & 1 & 1 \\ -2 & 0 & -2 \end{vmatrix} = -2 \neq 0. \quad (2.16)$$

Note that this choice is not necessarily unique since for instance

$$\det \begin{vmatrix} 3 & 1 & -3 \\ 0 & 0 & 1 \\ 0 & -2 & 0 \end{vmatrix} \neq 0. \quad (2.17)$$

## 2.5 Extended dimensional analysis

For slender structures, we will need to be careful when applying dimensional analysis because the intrinsic separation of length scales involved in the problem (*e.g.*, between thickness, width, total arc-length, or total dimension of the structure) can affect the dependent variables (*e.g.*, the critical buckling load) in different ways. This modified procedure is often referred to as **extended dimensional analysis**.<sup>3</sup>

Indeed, when considering a typical slender structure such as the beam shown in Fig. 2.1, we need to take into account the fact that it will deform along a *privileged direction* that is orthogonal to  $\hat{z}$ . As such, there is one length scale, the total arc-length of the beam, that dominates over the others. Such a structure is said to be *distorted*, in the sense that there are different types of interactions of physics phenomena across the different directions. Later in this course we will use energy methods to more precisely explore this difference in physical mechanism for elastic deformation in slender structures, for example, through the difference in bending versus stretching energies. Importantly, different geometric properties may affect the the modes of deformation in different ways; *e.g.*, radius vs. length in a rod, thickness vs. width or length of a plate, or thickness vs. radius of a spherical shell.

To address the problem at hand of a thin beam loaded axially (Fig. 2.1) using dimensional analysis, we will need to consider an extended base of length dimensions ( $L_r, L_z$ ) across the radius and the length of the beam, respectively, instead of a single base dimension ( $L$ ) as was done above in Example 2.2.2.

3: A more formal account of this topic can be found in the following book: H.E. Huntley 'Dimension analysis', New York, Dover (1967).

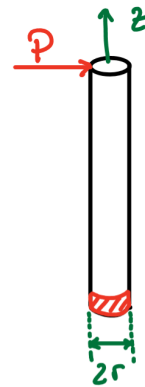


Figure 2.1: We need to consider an extended base of length dimensions

### Example 2.5.1 Load bearing capacity of a thin structure:

Consider a strength problem similar to the one above but for a thin parallelepipedic structure with 3 distinct length scales (see Fig. 2.2). We seek to compute the limit vertical load,  $P_{z, \text{lim}}$ , that the structure can take.

First, we introduce the extended system of base dimensions

$$(L_x, L_y, L_z, M, T), \tag{2.18}$$

where  $L_i$  denotes the length scale in the direction  $\hat{i}$  (with  $i = \{x, y, z\}$ ). The physical quantities of interest then be written as

$$\begin{aligned} [P_{z, \text{lim}}] &= L_z M T^{-2} \\ [H] &= L_z \\ [h] &= L_x \\ [b] &= L_y \\ [\sigma_0] &= [P_z] L_x^{-1} L_y^{-1} = L_x^{-1} L_y^{-1} L_z M T^{-2} \\ [\rho] &= L_x^{-1} L_y^{-1} L_z^{-1} M \\ [g] &= L_z T^{-2}. \end{aligned} \tag{2.19}$$

Following the same method for dimensional analysis that was dis-

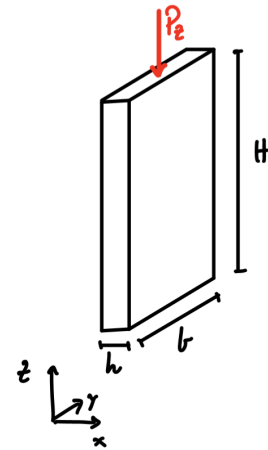


Figure 2.2:  $h < b \ll H$

cussed before, yields,

$$\Pi_0 = \frac{P_{z,lim}H}{b^2h\sigma_0} = F\left(\Pi_1 = \frac{Hg\rho}{\sigma_0} \equiv \mathcal{N}_{ga}\right), \quad (2.20)$$

where  $\mathcal{N}_{ga}$  is often referred to as the *Galileo's number*.

### Example 2.5.2 Load-bearing capacity of a horizontal slab under self-weight and mid-span loading:

Another example of a distorted structure is presented on Fig. 2.3. A slab of thickness  $h$ , width  $b$ , length  $l$ , and mass  $m$  is set horizontally and supported at two pins that are set apart by a distance  $l$ . The cross-sectional area of the slab is  $A = bh$ . The slab experiences self weight due to gravity. Since  $h \ll b < l$ , one length scale (the span,  $l$ ) dominates over others (the cross-sectional quantities,  $h$  and  $b$ ). The slab is loaded both by a force  $F_z$  at its mid-span and by self-weight.

As before, we want to find the load-bearing capacity

$$F_{z,lim} = f(l, b, h, \sigma_0, \rho, g), \quad (2.21)$$

by invoking the extended system of base dimensions. Even if the details of the calculation are left as an exercise, we make the following observations:

- ▶ The total number of parameters is  $7 = N + 1$ ;
- ▶ The rank of matrix of exponents is  $k = 5$ ;
- ▶ The number of dimensionless groups is  $N - k + 1 = 2$ ;
- ▶ We can pick  $(l, b, h, \sigma_0, g)$  as the basis of dimensionally independent variables.

Applying Buckingham- $\Pi$  theorem, we can obtain the following two dimensionless groups,  $\Pi_0$  and  $\Pi_1$ :

$$\Pi_0 = \frac{F_{z,lim}l}{bh^2\sigma_0} = F\left(\Pi_1 = \frac{gl^2\rho}{h\sigma_0}\right). \quad (2.22)$$

### Example 2.5.3 Euler buckling from dimensional analysis:

It is possible to compute an approximation the critical Euler buckling load from dimensional analysis alone (see Chapter 1). The various relevant quantities are presented in the schematic diagram of Fig. 2.4. Specifically, the length of the beam is  $l$ , its radius is  $r$ , the eccentricity (*i.e.*, imperfection) is  $e$ , the Young's modulus is  $E$  and the vertical applied load is  $P$ .

First, we note that buckling occurs when  $P > P_{cr}(l, e, r, E)$  and that the problem comprises  $N + 1 = 5$  parameters.

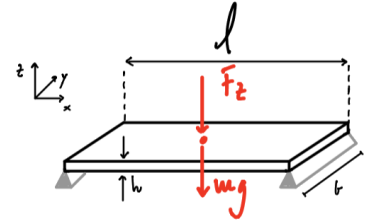


Figure 2.3: Pinned horizontal slab loaded at mid-span.  $h \ll b < l$

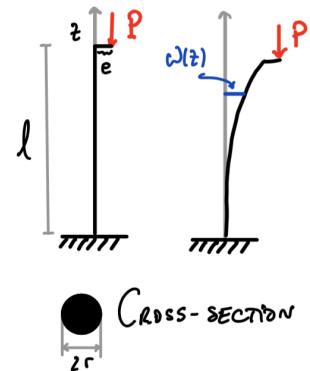


Figure 2.4: Euler buckling of beam.

The corresponding exponent matrix is

	$[P_{cr}]$	$[E]$	$[l]$	$[e]$	$[r]$
$M$	1	1	0	0	0
$L_r$	0	-4	0	1	1
$L_z$	1	3	1	0	0
$T$	-2	2	0	0	0

The rank of the exponent matrix is  $k = 3$ . We choose  $(l, r, E)$  as base to express the  $N - k + 1$  remaining parameters  $(P_{cr}, e)$  in dimensionless form. It can be shown that (the details of the calculation are left as an exercise) two dimensionless groups of this problem are:

$$\begin{aligned}\Pi_1 &= \frac{e}{r} \\ \Pi_0 &= \frac{P_{cr} l^2}{Er^4} = F(\Pi_1).\end{aligned}\quad (2.23)$$

Taking the limit of  $\frac{e}{r} \rightarrow 0$ , which corresponds to the case where the eccentricity (imperfection) of the beam  $e$  tends to zero, results in  $\Pi_1 \rightarrow 0$ . As such, in this limit,  $\Pi_1$  can be omitted. Finally, we have that

$$\lim_{\frac{e}{r} \rightarrow 0} \Pi_0 = \frac{P_{cr} l^2}{Er^4} = \text{constant}, \quad (2.24)$$

which is the Euler buckling condition that was presented in Chapter 1. As expected, the explicit relation is not known, and the value of the constant – the prefactor – must be obtained from a more detailed analysis, as was done in Chapter 1.

## 2.6 Physical similarity

Two systems or events are said to be *similar* if all dimensionless quantities have the same value. If two physical systems are similar, we first explore the behaviour of one (*e.g.*, the prototype) from the known behaviour of the other (*e.g.*, the model). This concept is extremely powerful in engineering design using prototypes and in precision model experiments constructed to study a phenomena away from its regular environment.

**Back to the above problem of beam bending:** Let us return to the problem solved in Example 2.5.2 but simplify it to consider only half of the mid-span (due to symmetry) and simplify the structure to a cylindrical beam of diameter  $h$  (instead of a slab), loaded at one of its extremities by a point load  $P$  that is set orthogonally to its arc-length. We consider two cases (1) and (2) by modifying the length is modified such that  $l^{(2)} = \lambda l^{(1)}$ , where the scaling factor  $\lambda$  is a positive real number and  $l^{(1)}$  is the original length. For both systems (1) and (2) to be similar, all dimensionless quantities must remain constant. One for the relevant dimensionless groups for this system, as in Eq. (2.22), is

$$\Pi_1 = \frac{\rho g l^2}{h \sigma_0}$$

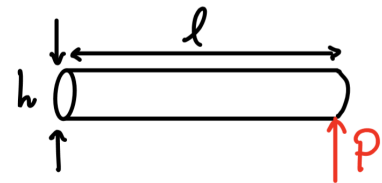
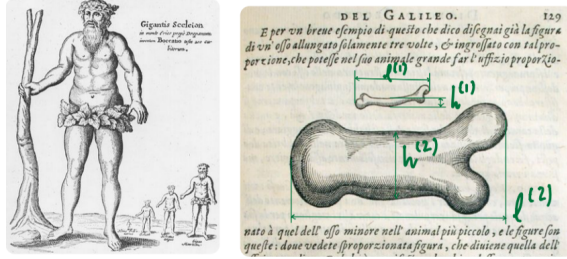


Figure 2.5: Initial cylinder



**Figure 2.6:** Drawing of the bones of a small (top) and a large (bottom) animals made by Galileo in his book *Two New Sciences*.

We ask: what must happen to the new diameter,  $h^{(2)}$  to ensure similarity, assuming that all other quantities remain fixed?

Imposing  $\Pi_1$  to be constant, we obtain

$$\frac{\rho g (l^{(1)})^2}{h^{(1)} \sigma_0} = \frac{\rho g (l^{(2)})^2}{h^{(2)} \sigma_0} \quad (2.25)$$

$$\frac{(l^{(1)})^2}{h^{(1)}} = \frac{\lambda^2 (l^{(1)})^2}{h^{(2)}}$$

from which it is evident that

$$\frac{h^{(2)}}{h^{(1)}} = \lambda^2 \quad (2.26)$$

Hence, if we triple the length,  $\lambda = 3$ , the thickness must be multiplied by a factor  $\frac{h^{(2)}}{h^{(1)}} = 9$ . This result rationalizes the observation made by Galileo in his *Two New Sciences* where he established a comparison between the femur of a human and that of a giant. Quoting Galileo:

“... I draw here the image of a bone increased only three times, but widened in such a way that it may perform, proportionally, in the giant animal, the same function the smaller bone performs in a small animal, and you can see how the augmented bone becomes out of proportion.”

In Fig. 2.6, we reproduce Galileo’s original drawing of the *giant animal* (bottom) and the *small animal*. Directly measurement of the lengths respective lengths from the image (using an image processing software) yields

$$\lambda_{\text{Galileo}} = \frac{l_{\text{Galileo}}^{(2)}}{l_{\text{Galileo}}^{(1)}} \approx 2.9 \quad \text{and} \quad \frac{h_{\text{Galileo}}^{(2)}}{h_{\text{Galileo}}^{(1)}} \approx 7.4 \quad (2.27)$$

For  $\lambda_{\text{Galileo}} \approx 2.9$ , the result from our scaling analysis in Eq. (2.26) predicts  $h^{(2)}/h^{(1)} \approx (2.9)^2 = 8.4$ , which is remarkably close to Galileo’s ‘prediction’ conveyed in his drawing! This result is striking since modern extended dimensional analysis was yet to be developed.

## 2.7 Scalings

Scaling analysis corresponds to the procedure followed to determine the interdependence of variables in a physical system, in a way that involves a combination of dimensional analysis and physical reasoning. Scaling



analysis often require a large degree of physical intuition, and can be very valuable in solving otherwise analytically intractable problems.

**Comment on notation:**

- ▶ The symbol " $\sim$ " means "scales as...".
- ▶ The symbols " $\approx$ ", " $\simeq$ " mean "approximately the same as...".

We will illustrate the power of scaling argument by addressing the following three specific problems:

**Scalings Problem 1: Why does a thin beam bend rather than shear?** (a scaling argument) From experience, we know that a clamped beam, when subjected to a vertical load at its free end, deforms through *bending* rather than *shearing*. We now seek to rationalize this observation through energy minimization and scalings.

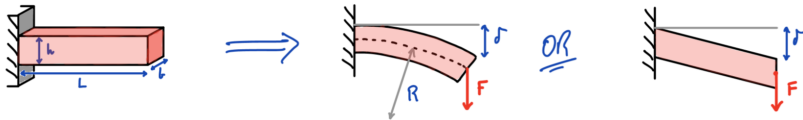


Figure 2.7: Will a slender beam bend or shear?

(i) *Bending case:* As it was shown in Eq. (1.2), the axial strain in a beam scales as:

$$\epsilon_{xx} \sim \frac{h}{R}, \quad (2.28)$$

where  $R$  is the radius of curvature, and from geometry (see Fig. 2.8),

$$\frac{1}{R} \sim \frac{\delta}{L^2}. \quad (2.29)$$

From Eq. (1.13), we finally get that

$$\mathcal{U}_{\text{bending}} \sim \frac{EIL}{R^2} \sim \frac{Eh^3b\delta^2}{L^3}. \quad (2.30)$$

(ii) *Shearing case:* The shear strain scales as:

$$\epsilon_{xy} \sim \frac{\delta}{L}, \quad (2.31)$$

and, thus, the shearing energy scales as

$$\mathcal{U}_{\text{shear}} \sim EA\epsilon_{xy}^2L \sim ELbh\left(\frac{\delta}{L}\right)^2. \quad (2.32)$$

Finally, the ratio between the bending and shearing energy scales as

$$\frac{\mathcal{U}_{\text{bending}}}{\mathcal{U}_{\text{shear}}} \sim \left(\frac{h}{L}\right)^2. \quad (2.33)$$

Consequently, if the beam is sufficiently slender (*i.e.*,  $\frac{h}{L} \ll 1$ ) shearing is energetically more costly and the beam will bend.

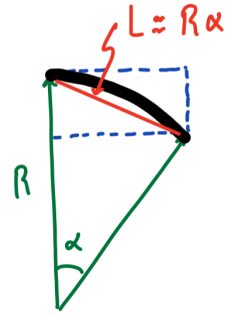


Figure 2.8:  $\delta = R(1 - \cos(\alpha)) \approx R(1 - 1 + \frac{\alpha^2}{2} + \dots) \approx \frac{R}{2} \cdot \frac{L^2}{R^2} \Rightarrow \frac{1}{R} = \kappa \approx \frac{d^2w}{dx^2} \sim \frac{\delta}{L^2}$

**Scalings Problem 2: Euler buckling through a scaling analysis:** Through scalings, we want to determine the critical buckling load,  $F_{cr}$ , of the beam represented on Fig. 2.9. The beam of length  $l$  is clamped at its bottom extremity and free at the other. A vertical force  $F$  and a horizontal force  $f$  are applied at the free end of the beam, such that its tip deflects by  $\delta$ . We are also interested in determining the effective spring stiffness  $K = f/\delta$  of the beam; *i.e.*, the spring constant in the horizontal direction.

From Eq. (1.7), we know that the internal moment scales as:

$$M \sim \frac{EI}{R} \sim EI \frac{\delta}{L^2}. \quad (2.34)$$

Furthermore, moment balance imposes

$$M = fL + F\delta. \quad (2.35)$$

Combining Eq. (2.34) and Eq. (2.35) we obtain:

$$f \sim \underbrace{\frac{1}{L} \left( \frac{EI}{L^2} - F \right)}_{=K} \delta \Rightarrow K \sim \frac{1}{L} \left( \frac{EI}{L^2} - F \right) \quad (2.36)$$

From the above result, we note that the effective spring stiffness of the beam vanishes,  $K \rightarrow 0$ , when the critical buckling load is approached,  $F_{cr} \approx EI/L^2$ . When this happens, the beam no longer presents resistance in the horizontal direction and buckling takes place. Moreover, the natural frequency of the beam,  $\omega = \sqrt{K/m}$ , where  $K$  is the effective spring stiffness of the beam and  $m$  is its mass, tends to zero in the vicinity of buckling.

**Scalings Problem 3: Buckling of an elastic strip under self weight:**

We seek to determine the maximum possible height,  $L_c$ , of a vertically clamped elastic strip, before it buckles under its self-weight. The gravitational energy of the structures scales as

$$\mathcal{U}_g \sim \rho g h b L_c^2, \quad (2.37)$$

and the bending energy scales as

$$\mathcal{U}_b \sim \frac{Eh^3b}{L_c^2} L_c. \quad (2.38)$$

At the onset of buckling, there is a balance between  $\mathcal{U}_g$  and  $\mathcal{U}_b$

$$U_g \sim U_b \Rightarrow \rho g h b L_c^2 \sim \frac{Eh^3b}{L_c^2} L_c, \quad (2.39)$$

, which yields a prediction for the critical length at which buckling occurs:

$$L_c \sim \left( \frac{Eh^2}{\rho g} \right)^{1/3} \quad (2.40)$$

This quantity  $L_c$  in Eq. (2.40) is often referred to as the elasto-gravity length scale. Note that, for a strip, the critical buckling conditions are independent of the width ( $L_c$  does not depend on  $b$ ). Elasticity dominates

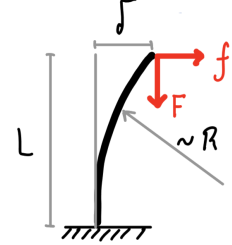


Figure 2.9: Slender beam undergoing buckling.

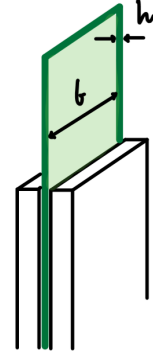


Figure 2.10: Elastic strip buckling under its own weight.

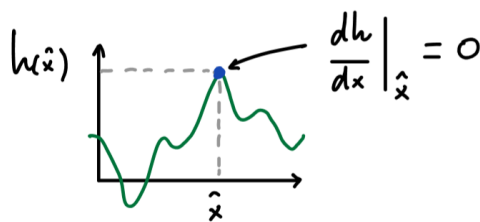
when  $L < L_c$  and the strip remains vertically straight. By contrast, when  $L > L_c$  gravity dominates and the strip buckles under its own weight. This scalings argument rationalizes why there are intrinsic limits to the height of tall structures (*e.g.*, trees, flag poles, towers). Therefore, to build taller structures, we need to increase their thickness or diameter in order to offer better resistance to buckling. All other parameters being constant, the maximum height that a structure can attain scales with its thickness to a power of  $2/3$ ; *i.e.*,  $L_c \sim h^{2/3}$ .



# 3 Calculus of Variations and Euler's Elastica

## 3.1 Preliminaries

Let us consider a *function* of one variable,  $h(x)$ .



- 3.1 Preliminaries . . . . . 24
- 3.2 Calculus of variations . . . . . 25
- 3.3 Calculus of variations with constraints . . . . . 26
- 3.4 Euler's Elastica . . . . . 30
  - Linearization of Euler's Elastica Equation: . . . . . 33
- 3.5 Numerical methods and examples . . . . . 36
- 3.6 Analytical methods to solve Euler's Elastica (elliptic integrals) 38

Figure 3.1: Simple 1-variable function

We can perform a Taylor expansion of  $h$  around the neighbourhood of interest (near the point  $\hat{x}$ ) to obtain,

$$\begin{aligned}
 h(x) &= h(\hat{x}) + \left. \frac{\partial h}{\partial x} \right|_{\hat{x}} (x - \hat{x}) + \left. \frac{\partial^2 h}{\partial (x - \hat{x})^2} \right|_{\hat{x}} \frac{h^2}{2} + \dots \\
 &= h(\hat{x}) + \mathcal{O}((x - \hat{x})^2)
 \end{aligned}
 \tag{3.1}$$

As we know from introductory calculus, a vanishing derivative,  $dh/dx$  evaluated at  $\hat{x}$ , signifies that, to first order, there is no variation in  $h$  for a small change in  $x$  in the neighborhood of  $\hat{x}$ .

**Example:** The ordinary differential equation

$$\frac{dh}{dx} = x^2 - 2x + 1 \tag{3.2}$$

has fixed points ( $dh/dx = 0$ ) at  $x = \pm 1$ .

### 3.2 Calculus of variations

We now turn to determining minima and maxima of a *function of a function*, which is called a *functional*. The underlying mathematical methodology is referred to as *Calculus of Variations*. Later in this course, this framework will be employed, for example, to compute the minimum of the elastic energy of a beam. The elastic energy is a functional given that it is a function of deflection, which is itself a function of position.

By way of example, consider the *function*  $h(x) : [0, 1] \rightarrow \mathbb{R}$ , with  $h(0) = 0$  and  $h(1) = 1$ , and the *functional*

$$F[h] = \frac{1}{2} \int_0^1 h'^2(x) dx, \quad (3.3)$$

where the square brackets,  $[\cdot]$ , as traditionally used to denote that  $F$  is, indeed functional. The *first variation of  $F$*  is defined as<sup>1</sup>

$$\begin{aligned} \delta F &= F[h + \delta h] - F[h] \\ &= \frac{1}{2} \int_0^1 (h' + \delta h')^2 dx - \frac{1}{2} \int_0^1 h'^2 dx \\ &= \frac{1}{2} \int_0^1 (2\delta h' h' + (\delta h')^2) dx \\ &\approx \int_0^1 h' \delta h' dx, \end{aligned} \quad (3.4)$$

1: Primed quantities  $(\cdot)'$  denote differentiation with respect to the underlying variable; e.g.,  $h' = dh/dx$ .

where, in the last step, we have neglected the  $(\delta h')^2$  term since it is of second order. Both  $h$  and  $h + \delta h$  must satisfy the boundary conditions (BCs), hence

$$h(0) = 0 \quad (3.5)$$

$$h(1) = 1 \quad (3.6)$$

$$\delta h(0) = 0 \quad (3.7)$$

$$\delta h(1) = 0 \quad (3.8)$$

Our task is to determine the functional form of  $h(x)$  satisfying the BCs in Eq. (3.5) and Eq. (3.6), such that  $\delta F[h + \delta h] = 0$  for any  $\delta h$ , which must itself satisfy Eq. (3.5) and Eq. (3.7). In other words, for all  $\delta h$  such that  $\delta h(0) = 0$  and  $\delta h(1) = 0$ , we have

$$\delta F[h + \delta h] = F[h + \delta h] - F[h] = \int_0^1 h' \delta h' dx = 0. \quad (3.9)$$

Integrating the above equations by parts, yields

$$0 = [h' \delta h]_0^1 - \int_0^1 h'' \delta h dx = 0 \Rightarrow \int_0^1 h'' \delta h dx = 0. \quad (3.10)$$

Since Eq. (3.10) must hold for any variation  $\delta h$ , it can only be true *if and only if*  $h'' = 0$ . Recalling the boundary conditions  $h(0) = 0$  and  $h(1) = 1$ , we finally obtain the unique solution  $h(x) = x$ .

**Example 3.2.1 Shortest path between two points**

Consider two paths,  $h(x)$  and  $h(x) + \delta h(x)$ , between two points,  $x_1$  and  $x_2$ , with  $x_1 \leq x \leq x_2$ . First, we assume that the difference between the two paths is small; *i.e.*,  $\delta h(x) \ll h(x)$ . The length of the path  $h(x)$ , a functional, is

$$L[h(x)] = \int_{x_1}^{x_2} ds = \int_{x_1}^{x_2} dx \sqrt{1 + h'^2}. \tag{3.11}$$

For small slopes ( $h' \ll 1$ ):  $\sqrt{1 + h'^2} \approx \frac{1}{2}h'^2$ . Under this approximation, our problem translates into the minimization of

$$L[h(x)] = \int_{x_1}^{x_2} \frac{h'^2}{2} dx, \tag{3.12}$$

which is similar to what we solved above (the two problems have the same solution), but with different boundary conditions. The final answer is a *straight line*,

$$h(x) = ax + b, \tag{3.13}$$

where  $a$  and  $b$  depend on the values of  $x_1$  and  $x_2$ . Note that the solution in Eq. (3.13) must be a minimum since no maximum exists.

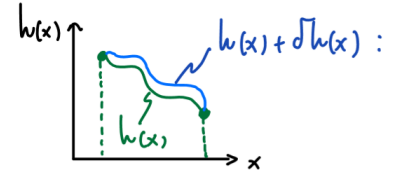


Figure 3.2: Path (green) and variation (blue)

### 3.3 Calculus of variations with constraints

Next, we extend the variational framework presented above for cases when the problem must satisfy a series of constraints. We seek to minimize  $f(x, y)$  subject to the constraint  $\phi(x, y) = 0$ . To do so, it suffices to minimize the alternative quantity  $h(x, y) = f(x, y) + \lambda\phi(x, y)$  ( $\lambda$  is referred to as a *Lagrange multiplier*), as we demonstrate next.

Suppose that a constraint  $\phi(x, y) = 0$  allows us to define  $y = g(x)$ , and  $f(x, y) = f(x, g(x))$ . Maximization or minimization of  $f(x, y)$  can then be expressed as

$$\frac{\partial f(x, y)}{\partial x} = 0 \tag{3.14}$$

which be rewritten as<sup>2</sup>

$$\frac{\partial f}{\partial x} + \frac{\partial f}{\partial y} \frac{\partial y}{\partial x} = f_x + f_y g' = 0. \tag{3.15}$$

Furthermore, differentiating  $\phi(x, y) = 0$  with respect to  $x$  gives

$$\phi_x + \phi_y g' = 0 \iff g' = -\frac{\phi_x}{\phi_y} \tag{3.16}$$

2: Here, the subscripts  $(\cdot)_x$  and  $(\cdot)_y$  represent partial differentiation with respect to  $x$  and  $y$ . Note that later in this course, once we start dealing with the components of tensorial quantities (*e.g.*,  $\sigma_{xx}$ ), we will have to update this notation to avoid confusions with subscripts. For example,  $\sigma_{xx,y}$  will represent the partial derivative of the  $xx$  component of the tensor  $\sigma$  with respect to the variable  $y$ . For now, the usage of a comma to denote partial derivatives is omitted, for simplicity.

with  $\phi_y \neq 0$ .

Substituting Eq. (3.16) into Eq. (3.15), yields

$$f_x - f_y \frac{\phi_x}{\phi_y} = 0, \quad (3.17)$$

and a similar expression can be obtained for  $f_y$ . Now, we define the ratio  $\lambda = -f_y/\phi_y$ , which allows us to write

$$\begin{aligned} f_y + \lambda\phi_y &= 0 \\ f_x + \lambda\phi_x &= 0. \end{aligned} \quad (3.18)$$

In summary, minimizing  $f(x, y)$  with the constraint  $\phi(x, y) = 0$  is equivalent to solving the system in Eqs. (3.18). Had we chosen to minimize  $h(x, y) = f(x, y) + \lambda\phi(x, y)$ , we would have arrived at

$$\begin{cases} \frac{\partial h}{\partial x} = 0 \\ \frac{\partial h}{\partial y} = 0 \end{cases} \Rightarrow \begin{cases} f_x + \lambda\phi_x = 0 \\ f_y + \lambda\phi_y = 0 \end{cases}, \quad (3.19)$$

which is the same as Eqs. (3.18).

In summary, to minimize  $f(x, y)$  subject to a constraint  $\phi(x, y) = 0$ , it suffices to minimize  $h(x, y) = f(x, y) + \lambda\phi(x, y)$ , where  $\lambda$  is a *Lagrange multiplier*.

### Example 3.3.1 Equilibrium shape of a bent beam clamped at its ends

An elastic beam (of total arclength  $l$ , width  $b$ , and thickness  $h$ ) is clamped at two points ( $x = 0$  and  $x = L$ ) that are separated by a horizontal distance  $L$  (see Fig. 3.3). At this clamping points, the deflection of the beam,  $w(x)$ , vanishes:  $w(x = 0) = 0$  and  $w(x = L) = 0$ . The beam has an areal moment of inertia  $I = bh^3/12$  and is made out of material with Young's modulus  $E$ .

We seek to determine the shape of the beam, such as its elastic energy is minimized, under the constraint that its total arc-length is  $l$ ; that is

$$l = \int_0^L ds = \int_0^L dx \sqrt{1 + \left(\frac{dw}{dx}\right)^2}. \quad (3.20)$$

We will solve this optimization problem using calculus of variations, with the constraint stated above.

As we saw in Chapter 1, the total bending energy of the beam is

$$u_b = \frac{1}{2}EI \int_0^L \left(\frac{d^2w}{dx^2}\right)^2 dx, \quad (3.21)$$

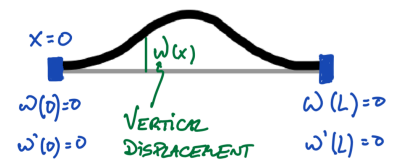


Figure 3.3: width:  $b$ , thickness:  $h$ , Young's modulus:  $E$ , moment of inertia:  $I = \frac{bh^3}{12}$

and the energy functional that we seek to minimize is thus

$$\mathcal{U}_b[w(x)] = \int_0^L \left\{ C \left( \frac{d^2 w}{dx^2} \right)^2 - \lambda \sqrt{1 + \left( \frac{dw}{dx} \right)^2} \right\} dx, \quad (3.22)$$

where  $C = EI/2$  is a constant and  $\lambda$  is a Lagrange multiplier. If we now consider a perturbation  $\delta w$  of the deflection (shape), the first variation of the energy is

$$\begin{aligned} \delta \mathcal{U}_b &= \mathcal{U}_b[w + \delta w] - \mathcal{U}_b[w] \\ &= \int_0^L \left\{ C \left( \frac{d^2(w + \delta w)}{dx^2} \right)^2 - \lambda \sqrt{1 + \left( \frac{d}{dx}(w + \delta w) \right)^2} \right\} dx - \mathcal{U}_b[w]. \end{aligned} \quad (3.23)$$

The above expression for  $\mathcal{U}_b$  can be simplified by only retaining the leading-order terms to read:

$$\begin{aligned} \delta \mathcal{U}_b &= \mathcal{U}_b[w + \delta w] - \mathcal{U}_b[w] \\ &= \int_0^L \left\{ 2C \underbrace{\frac{d^2 w}{dx^2} \frac{d^2 \delta w}{dx^2}}_{\equiv \mathcal{J}} - \lambda \frac{dw}{dx} \frac{d\delta w}{dx} \right\} dx. \end{aligned} \quad (3.24)$$

The integral of the first term,  $\mathcal{J}$ , in the equation above, can be integrated by parts to obtain

$$\mathcal{J} = \int \frac{d^2 w}{dx^2} \frac{d^2 \delta w}{dx^2} dx = \left[ \frac{d^2 w}{dx^2} \frac{d\delta w}{dx} \right]_0^L - \int_0^L \frac{d\delta w}{dx} \frac{d^3 w}{dx^3} dx. \quad (3.25)$$

Introducing this result into Eq. (3.24) and simplifying leads to

$$\begin{aligned} \delta \mathcal{U}_b &= - \int_0^L \left\{ 2C \frac{d^3 w}{dx^3} + \lambda \frac{dw}{dx} \right\} \frac{d\delta w}{dx} dx \\ &= -[u\delta w]_0^L - \int_0^L \frac{d}{dx} \left\{ 2C \frac{d^3 w}{dx^3} + \lambda \frac{dw}{dx} \right\} \delta w dx \equiv 0, \end{aligned} \quad (3.26)$$

which must vanish for all possible variation  $\delta w$ . Hence,

$$\frac{d}{dx} \left\{ 2C \frac{d^3 w}{dx^3} + \lambda \frac{dw}{dx} \right\} = 0 \Rightarrow 2C \frac{d^2 w}{dx^2} + \lambda w = C_1 x + C_2. \quad (3.27)$$

The general solution of the above ODE is

$$w(x) = A \cos \left( \sqrt{\frac{\lambda}{2C}} x + \phi \right) + C_1 x + C_2 \quad (3.28)$$

where the constants of integration,  $\phi$ ,  $C_1$  and  $C_2$ , are to be determined by applying the appropriate boundary conditions. By imposing the zero-displacement condition at the left end, *i.e.*  $w(0) = 0$ , we find  $C_2 = -A \cos \phi$ . The clamped condition at the same end,  $w'(0) = 0$ , allows



us to write  $C_1 = A\sqrt{\lambda/2C} \sin \phi$ . We pursue by imposing the boundary conditions at the right end, at  $x = L$ . The relation  $w(L) = 0$  yields:

$$A \cos \left( \sqrt{\frac{\lambda}{2C}} L + \phi \right) - A \cos \phi + C_1 L = 0. \quad (3.29)$$

Next, the relation  $w'(L) = 0$ , on the other hand, gives us

$$A \sqrt{\frac{\lambda}{2C}} \left[ -\sin \left( \sqrt{\frac{\lambda}{2C}} L + \phi \right) + \sin \phi \right] = 0. \quad (3.30)$$

Eq. (3.30) must be satisfied for any value of  $\phi$ , which induces  $\sqrt{(\lambda/2C)}L = 2\pi$ , or, rearranging,

$$\lambda = \frac{8C\pi^2}{L^2}. \quad (3.31)$$

Recalling that we defined  $C = \frac{EI}{2}$ , we find  $\lambda = 4\pi^2 EI/L^2$ , which has dimensions of force. We deduce that, for the current problem, the Lagrange multiplier  $\lambda$  represents the force that the clamp must apply to the beam in order to maintain the imposed shape.

Finally, after replacing  $\lambda$  into Eq. (3.29), we obtain  $C_1 = 0$  and  $\phi = \pi$ . We find the shape of the deformed beam:

$$w(x) = A \left[ 1 - \cos \left( \frac{2\pi x}{L} \right) \right]. \quad (3.32)$$

The equilibrium shape of the deformed beam displays a cosine profile, this is an important statement we could not make previously, neither in Chapter 1 (linear beams) nor in Chapter 2 (dimensional analysis).

To determine the last integration constant  $A$  (the maximum deformation at the mid-span of the beam,  $w(x = L/2)$ ), we invoke the length constraint; *i.e.*, the total arclength of the deformed beam must be equal to the undeformed length  $l$ . Hence, we can write

$$\begin{aligned} l &= \int_0^L ds = \int_{-L}^L \sqrt{1 + w'^2} dx \approx \int_0^L \left( 1 + \frac{1}{2} w'^2 \right) dx \\ \Rightarrow A &\approx \pm \frac{1}{\pi} \sqrt{L(l - L)} \end{aligned} \quad (3.33)$$

where we assumed that the beam only undergoes small rotation (*i.e.*, slopes are small, hence the  $\approx$  sign) and we also used the standard trigonometric integral  $\int_0^L \sin^2(2\pi x/L) dx = L/2$ .

More complex shapes (higher order modes) can be obtained with additional constraints. For example, in Fig. 3.4, we present a schematic diagram of an elastic beam that is forced to deform between two parallel undeformable walls, separated by a distance  $H$ . In this setup, as the extremities of the elastic beam are brought closer from an initially straight configuration, buckling first occurs in the first mode. However, as we continue bringing the extremities closer, the amplitude of the deformed beam profile reaches the distance between between the two walls. At this stage, the beam becomes in contact with the top and bottom walls and snap successively into a higher-order buckling modes. At large buckling modes, the beam will display a "wrinkled" pattern, as shown in the

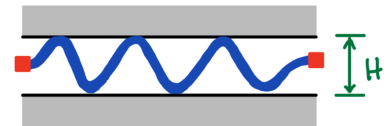


Figure 3.4: Buckling with lateral constraints

schematic.

Returning to the earlier case without constraining walls (see Fig. 3.5), when the extremities of the elastic beam are brought together at a smaller distance  $L$ , slopes are no longer locally small (*i.e.*, local rotations become significant) and the first order approximation we used in Eq (3.33) is no longer valid. Instead of the sinusoidal shape that we computed in Example 3.3.1, we obtain nonlinear shapes (see Fig. 3.5). To compute the shapes of this case of an inextensible beam under large rotations, we need to modify the energy functional to account for non-linear beam profiles, which is addressed in the next section.

### 3.4 Euler's Elastica

We now consider an inextensible elastic beam, clamped at one end, with a load,  $\mathbf{P} = (P_x, -P_y)$ , applied at its free . This beam represents the centerline of a 3D body, and will be considered as an inextensible elastic curve. Furthermore, let us denote the arc-length coordinate by  $s$ , and the local angle between the tangent of the curve and  $\hat{x}$  by  $\theta(s)$ . The bending stiffness of this beam is  $EI$  and its total arc-length is  $L$ . In Fig. 3.6, we provide a schematic diagram of this problem and define the relevant variables.

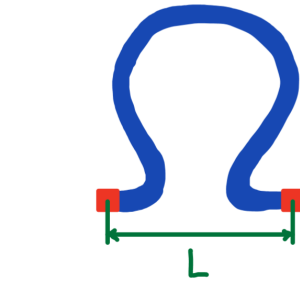
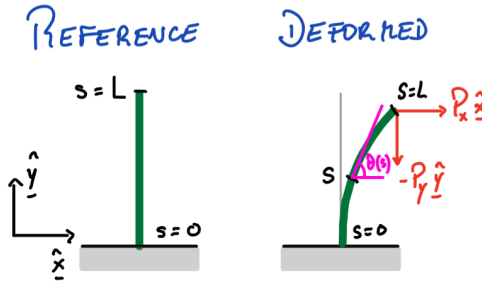


Figure 3.5: How do we go about analysing these cases of large rotations, when the deformation becomes significantly non-linear?

Figure 3.6: Elastic curve with bending stiffness  $EI$

We aim at determining the equilibrium shape of this elastic curve, under the boundary conditions  $x(s = 0) = 0, y(s = 0) = 0, \theta(s = 0) = \frac{\pi}{2}$ , while allowing for finite (*i.e.*, not small) rotations. Importantly, the inextensibility assumption implies that the axial strain  $\epsilon_{ss} = 0$ , and the bending curvature can be written as  $\kappa(s) = d\theta/ds = \theta'(s)$ . Contrary to the problems discussed in the previous section, we are now dealing with nonlinear kinematics, since  $\theta$  is not necessarily small.

As a first step to solve this problem, we write the Lagrangian coordinates, With respect to the initial configuration, of the centerline of the beam as

$$\begin{cases} x'(s) = \cos \theta \\ y'(s) = \sin \theta \end{cases} \quad (3.34)$$

**Energetics:** The bending energy of the system under investigation can be written as the functional,

$$\mathcal{U}_b[\theta(s)] = \frac{1}{2} \int_0^L EI \kappa^2(s) ds = \frac{1}{2} \int_0^L EI (\theta'(s))^2 ds, \quad (3.35)$$

where  $\kappa(s) = d\theta/ds = \theta'(s)$  is the local curvature of the structure at a particular point  $s$  along its arc-length. The external potential energy (the potential energy of the external forces, *i.e.*, the negative of the work done by these load located at  $s = L$ ) is

$$\begin{aligned} \mathcal{U}_p(P_x, P_y; \theta(s)) &= -P_x x(L) + P_y y(L) \\ &= \int_0^L (-P_x \cos(\theta(s)) + P_y \sin(\theta(s))) ds. \end{aligned} \quad (3.36)$$

The bending energy and the external potential energy can now be combined to write the total energy functional as,

$$\begin{aligned} \mathcal{U}_{\text{tot}} &= U_b(\theta(s)) + U_p(P_x, P_y; \theta(s)) \\ &= \int_0^L \left\{ \frac{EI}{2} (\theta'(s))^2 - P_x \cos(\theta(s)) + P_y \sin(\theta(s)) \right\} ds \end{aligned} \quad (3.37)$$

Obtaining the equilibrium configuration of the beam requires the computation of the first variation of energy, which must vanish at equilibrium, for any perturbation of the shape of the beam,  $\delta\theta(s)$ :

$$\delta\mathcal{U}_{\text{tot}} = \mathcal{U}_{\text{tot}}(\theta + \delta\theta) - \mathcal{U}_{\text{tot}}(\theta) = 0. \quad (3.38)$$

The bending energy of the perturbed shape is:

$$\begin{aligned} \mathcal{U}_b(\theta + \delta\theta) &= \frac{1}{2} \int_0^L EI (\theta' + \delta\theta')^2 ds \\ &= \underbrace{\frac{1}{2} \int_0^L EI \theta'^2 ds}_{\mathcal{U}_b(\theta)} + \underbrace{\int_0^L EI \theta' \delta\theta' ds}_{\delta\mathcal{U}_b} + \mathcal{O}((\delta\theta')^2), \end{aligned} \quad (3.39)$$

Similarly, we get the following result for the external potential energy:

$$\mathcal{U}_p(\theta + \delta\theta) = \mathcal{U}_p(\theta) + \underbrace{\int_0^L (P_x \sin \theta + P_y \cos \theta) \delta\theta ds}_{\delta\mathcal{U}_p}, \quad (3.40)$$

where we used the fact that  $\cos(\theta + \delta\theta) = \cos \theta + (\cos \theta)' \delta\theta + \dots$ , and  $\sin(\theta + \delta\theta) = \sin \theta + (\sin \theta)' \delta\theta + \dots$  by expansion of the two trigonometric functions.

The first variation of the total energy is thus

$$\int_0^L \{ (EI\theta') \delta\theta' + (P_x \sin \theta + P_y \cos \theta) \delta\theta \} ds = 0 \quad (3.41)$$

where  $\delta\theta$  represents kinematically admissible rotations such that  $\delta\theta(0) = 0$  (any perturbation of the shape must vanish at the clamped end). The result in Eq. (3.41) is referred to as the *weak form* of the problem.

**Equilibrium equations:** Our goal is now to start from the weak formulation of the problem stated in Eq. (3.41) to obtain the governing

equilibrium equations. As a first intermediate step, we integrate by parts the first term of Eq. (3.41), as

$$\int_0^L (EI\theta') \frac{d(\delta\theta)}{ds} ds = [(EI\theta') \delta\theta]_0^L - \int_0^L \delta\theta (EI\theta')' ds = 0. \quad (3.42)$$

Note that  $[(EI\theta') \delta\theta]_0^L = 0$ , because  $EI\theta'(L) = M(L) = 0$  since there is no applied moment at the free-end, and  $EI\theta'(0)\delta\theta(0) = 0$  since  $\delta\theta(0) = 0$ . Hence, we can write

$$\int_0^L \delta\theta (EI\theta')' ds = 0, \quad (3.43)$$

We now substitute this result in Eq. (3.41) into Eq. (3.41):

$$\int_0^L (EI\theta'' - P_x \sin \theta - P_y \cos \theta) \delta\theta ds = 0, \quad (3.44)$$

where we have assumed that the bending stiffness is constant<sup>3</sup> (independent of  $s$ ). As above, we recognize that Eq. (3.44) must hold for any perturbation of the shape  $\delta\theta$ , which can only be satisfied if:

$$EI\theta''(s) - P_x \sin \theta - P_y \cos \theta = 0. \quad (3.45)$$

3: Note that this may not always be the case!  $EI$  could be a function of  $s$  if the beam was tapered with  $I = \hat{I}(s)$  or if it had a spatially varying Young's modulus with  $E = \hat{E}(s)$ , or both

The result in Eq. (3.45) is often referred to as **Euler's Elastica Equation** for inextensible elastic beams (in this case specialized with a load  $\mathbf{P}$  applied at its free tip) and represents the *strong form* of the problem. This is nonlinear ordinary differential equation that can be solved given boundary conditions. An alternative way to interpret Eq. (3.45) is to recognize that it expresses moment balance of the inextensible elastic beam, which may be easier to visualize if we rewrite it as

$$M'(s) - P_x \sin \theta - P_y \cos \theta = 0. \quad (3.46)$$

In fact, we could have more readily obtained the equation above, directly from moment balance, as we perform next by making use of the schematic diagram shown in Fig. 3.7

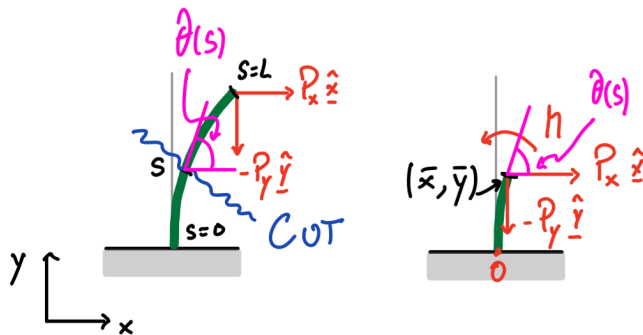


Figure 3.7: Same problem with moment balance.

We recall that  $(\bar{x}(s), \bar{y}(s))$  with  $d\bar{x}/ds = \bar{x}' = \cos \theta$  and  $d\bar{y}/ds = \bar{y}' = \sin \theta$ . Balance of moments at point  $s$ , with respect to about the clamp at

point  $O$  gives

$$\begin{aligned} M(s) - P_x \bar{y} - P_y \bar{x} &= 0 \\ M'(s) - P_x \bar{y}' - P_y \bar{x}' &= 0 \end{aligned} \quad (3.47)$$

and finally

$$M'(s) - P_x \sin \theta - P_y \cos \theta = 0, \quad (3.48)$$

which is the same result that we had obtained above using the variational approach. The fact that we arrived at the same result having followed two different routes should not be surprising, since the conditions that minimize the total energy are identical to imposing equilibrium. This observation is the foundation of the **Principle of Virtual Work**, of which we will make extensive use throughout this course.

### Linearization of Euler's Elastica Equation:

Our goal is now to recover the result that we had obtained previously for the cases of small slopes (rotations) and small deflection. To do so, we will linearize Eq. (3.45). It is expected that we should find the classic and familiar cantilever beam solution from Chapter 1; *i.e.*, the linear regime of Euler-Bernoulli description of elastic beams under small deflections.

First, we introduce a small perturbation parameter  $\eta$ , representing an infinitesimally small deviation from the straight shape of the beam. The quantities of interest, the local angle  $\theta$ , and the components of the applied load,  $P_x$  and  $P_y$ , can now be written as an expansion at different orders in  $\eta^4$ :

$$\begin{aligned} P_x &\rightarrow 0 + \eta P_x \\ P_y &\rightarrow 0 + \eta P_y \\ \theta &\rightarrow \theta_0 - \eta \theta_1 \end{aligned} \quad (3.49)$$

4: Since  $\eta$  is a small parameter, we neglect any terms of order higher than  $\mathcal{O}(\eta^2)$

Introducing these perturbed parameters expressed in Eq. (3.49) into Eq. (3.45), we obtain

$$EI (\theta_0'' - \eta \theta_1'') - \eta P_x (\sin \theta_0 + \cos \theta_0 \cdot \eta \theta_1) - \eta P_y (\cos \theta_0 - \sin \theta_0 \cdot \eta \theta_1) = 0. \quad (3.50)$$

Collecting all the zero-order terms (*i.e.*; those that do not depend on  $\eta$ ), yields

$$EI \theta_0'' = 0, \quad (3.51)$$

with boundary conditions

$$\left. \begin{aligned} \theta_0(0) &= \pi/2 \\ \theta_0'(L) &= 0 \end{aligned} \right\}. \quad (3.52)$$

Therefore,  $\theta_0(s) = \pi/2$  is the trivial solution, corresponding to a vertically straight beam that is undeformed.

At first order and neglecting higher-order terms, the ODE to solve is:

$$EI \theta_1'' + P_x = 0, \quad (3.53)$$

with boundary conditions

$$\left. \begin{array}{l} \theta_1(0) = 0 \\ \theta_1'(L) = 0 \end{array} \right\} \quad (3.54)$$

Note that  $\cos \theta_0 = 0$  because the beam is clamped. Hence,  $\theta_0 = \pi/2$ .

leading to the first-order solution:

$$\theta_1(s) = \frac{P_x}{EI} s(L-s), \quad (3.55)$$

which is an expression for the perturbed angle as a function of the arc-length. Note that  $\theta_1' = \frac{P_x}{EI}(L-2s)$ , and since  $M(s) = EI\theta'$ , the largest moment is found at the clamped end where  $s = 0$ , as expected.

**Shape of linearized solution:** We can determine the deflection anywhere along the arc-length from the linearized solution. Let us take  $x$  and  $y$  to be the coordinates of a *slight* perturbation of the straight solution (up to first-order):

$$\left\{ \begin{array}{l} y = y_0 + \eta y_1 \\ x = x_0 + \eta x_1 \end{array} \right. \quad (3.56)$$

Differentiation of these coordinates, with  $x' = dx/ds$  and  $y' = dy/ds$ , yields:

$$\rightarrow \left\{ \begin{array}{l} y' = y_0' + \eta y_1' \\ x' = x_0' + \eta x_1' \end{array} \right. \quad (3.57)$$

From the kinematic assumptions, we get

$$\begin{aligned} y'(s) &= \sin \theta = \sin(\theta_0 - \eta\theta_1) \\ &= \sin \theta_0 \underbrace{\cos(\eta\theta_1)}_{\approx 1} - \cos \theta_0 \underbrace{\sin(\eta\theta_1)}_{\approx \eta\theta_1} \\ &= \sin \theta_0 - \cos \theta_0 \cdot \eta\theta_1, \end{aligned} \quad (3.58)$$

and

$$\begin{aligned} x'(s) &= \cos \theta = \cos(\theta_0 - \eta\theta_1) \\ &= \cos \theta_0 \underbrace{\cos(\eta\theta_1)}_{\approx 1} + \sin \theta_0 \underbrace{\sin(\eta\theta_1)}_{\approx \eta\theta_1} \\ &= \cos \theta_0 + \sin \theta_0 \cdot \eta\theta_1. \end{aligned} \quad (3.59)$$

Collecting the zero-order terms, we get

$$\left\{ \begin{array}{l} y_0' = \sin \theta_0 \\ x_0' = \cos \theta_0 \end{array} \right. \quad (3.60)$$

Similarly, collecting the first-order terms, and recalling both Eq. (3.55) and the straight-solution result  $\theta_0 = \pi/2$ , we get

$$\left\{ \begin{array}{l} y_1' = 0 \\ x_1' = \frac{P_x}{EI} s(L-s) \end{array} \right. \quad (3.61)$$

Integration of the zeroth-order terms gives

$$y_0(s) = \underbrace{\sin \theta_0}_{=1} \int_0^s d\tilde{s} = s, \quad (3.62)$$

which is simply the vertical coordinate, and

$$x_0(s) = 0, \quad (3.63)$$

because the solution is straight at the zeroth order. Similarly for the first order terms, integration gives

$$y_1(s) = 0, \quad (3.64)$$

and

$$x_1(s) = \frac{P_x}{EI} \left( \frac{s^2}{2} L - \frac{s^3}{6} \right), \quad (3.65)$$

which is the solution for a clamped beam under pure bending, assuming small strains and deformation. We could have obtained this result easily from force methods, as was done in Chapter 1 by invoking balance of the internal forces.

We can make the following remarks:

1. The result  $y_1(s) = 0$  is a direct consequence of inextensibility.
2. The transverse stiffness of this cantilevered beam is

$$K_x = \frac{P_x}{x_1(L)} = \frac{P_x}{\frac{P_x}{EI} \left( \frac{L^3}{2} - \frac{L^3}{6} \right)} = \frac{3EI}{L^3}, \quad (3.66)$$

which is a result we had already obtained in Chapter 1.

3. On the other hand, the axial stiffness is

$$K_y = \frac{P_y}{y_1(L)} = \infty, \quad (3.67)$$

which is also a consequence of the inextensibility condition.

**Dimensionless equations:** We start by identifying relevant scales, as  $s^* = x^* = y^* = L$  (length of the elastica),  $\theta^* = 1$ . Also, from the moment-curvature relation,  $M^* \sim EI \frac{\theta^*}{s^*}$ , leading to  $M^* = \frac{EI}{L^*}$ , and  $P^* = \frac{M^*}{L^*} = \frac{EI}{L^{*2}}$ .

From there we derive the dimensionless quantities  $\bar{x} = \frac{x}{L} = \frac{x^*}{L^*}$ ,  $\bar{s} = \frac{s}{L}$ ,  $\bar{P}_x = \frac{P_x L^2}{EI}$ ,  $\bar{P}_y = \frac{P_y L^2}{EI}$ . Let us be careful with the angle, since  $\bar{\theta}(\bar{s}) = \frac{\theta(s)}{\theta^*}$  and  $\bar{\theta}(\bar{s}) = \theta(s)$  leads to

$$\bar{\theta}(\bar{s}) = \theta(L\bar{s}) \Rightarrow \begin{cases} \theta'(s) = \frac{1}{L} \bar{\theta}'(\bar{s}) \\ \theta''(s) = \frac{1}{L^2} \bar{\theta}''(\bar{s}) \end{cases}. \quad (3.68)$$

Finally, we get the following dimensionless equation for  $\theta(s)$

$$\begin{aligned} \frac{EI}{L^2} \bar{\theta}''(\bar{s}) - \frac{EI}{L^2} \bar{P}_x \sin \bar{\theta}(\bar{s}) - \frac{EI}{L^2} \bar{P}_y \cos \bar{\theta}(\bar{s}) &= 0 \\ \Rightarrow \bar{\theta}''(\bar{s}) - \bar{P}_x \sin \bar{\theta}(\bar{s}) - \bar{P}_y \cos \bar{\theta}(\bar{s}) &= 0, \end{aligned} \quad (3.69)$$

that must be satisfied by the following boundary conditions:

$$\left. \begin{aligned} \bar{\theta}(0) &= \frac{\pi}{2} \\ \bar{\theta}'(1) &= 0 \end{aligned} \right\}. \quad (3.70)$$

This dimensionless ODE for  $\theta(s)$  in Eq. (3.68) cannot, in general, be solved analytically. However, computational techniques allow us to compute numerical solutions of  $\bar{\theta}(s)$  under prescribed boundary conditions.

### 3.5 Numerical methods and examples

Analytically solving the ODE presented in Eq. 3.69 under the boundary conditions specified in Eqs. 3.70 results in highly non-trivial solutions (we will present analytical procedures in the following section). Alternative methods, enabled by the increasing computational performance over the past few decades (unavailable at the time of Euler!), enable us to solve such ODE's numerically. In this section, we describe a typical numerical solving procedure; the **shooting method**.

First, we must realize that our system of ODE with boundary conditions corresponds to a Boundary Value Problem (BVP), *i.e.* boundary conditions are imposed at both ends of the beam (at  $\bar{s} = 0$  and  $\bar{s} = 1$ ). Since boundary conditions are not only imposed at the clamped end of the beam (at  $\bar{s} = 0$ ), we do not have all the ingredients to integrate the differential equation for  $\theta(s)$  along  $s$ . Indeed, a second order ODE requires two *initial* conditions to be numerically integrated.

To circumvent the difficulty mentioned above to integrate our ODE, we rewrite the boundary conditions by discarding the condition at the free end of the beam. Instead, we provide a first guess for the term  $\bar{\theta}'(0)$ , such that  $\theta'(0) = a$ . By providing a second initial boundary condition, we have converted our problem into an Initial Value Problem (IVP), for which we can numerically integrate our ODE. The goal of the shooting method is to find the parameter  $a$  for which the integrated solution of  $\bar{\theta}(s)$  provides the actual target boundary condition; *i.e.*  $\bar{\theta}(1) = 0$ . Solving for the *guessed* parameter  $a$  is typically performed numerically using a Newton-Raphson root-finding algorithm, whose goal is to provide successively improved values of  $a$ . Once the parameter  $a$  which satisfies  $\bar{\theta}'(1) = 0$  is found, the integration of the ODE under this correct initial condition provides the final solution for  $\bar{\theta}(\bar{s})$ .

In summary, the main steps of the shooting methods are as follows:

1. We first define the problem  $P(a, \bar{P}_x, \bar{P}_y)$ :

$$\left\{ \begin{aligned} \bar{\theta}'' - \bar{P}_y \cos \bar{\theta} - \bar{P}_x \sin \bar{\theta} &= 0 \\ \bar{\theta}(0) = 0, \bar{\theta}'(0) &= a \end{aligned} \right. \quad (3.71)$$

2. We have transformed our BVP into an IVP.
3. We integrate the ODE using a conventional numerical solver.
4. We define the function shoot  $(\bar{P}_x, \bar{P}_y, a) = \theta'(1)$
5. Iteratively solve for  $a$  such that shoot  $(\bar{P}_x, \bar{P}_y, a) = 0$ . This step is typically performed using a Newton-Raphson root-find algorithm.



In Fig. 3.8 and Fig. 3.9, we provide examples of numerical solutions of the cantilever beam problem that was addressed in Section 3.4.

In Fig. 3.8, the loading force is directed along the horizontal axis, *i.e.*  $\bar{P}_y = 0$ . Note that in this case of a horizontal loading, the relation of the tip horizontal displacement as a function of the load  $\bar{P}_x$  can be approximated by the linear prediction of Eq. 3.65 for small values of  $\bar{P}_x$  (red line).

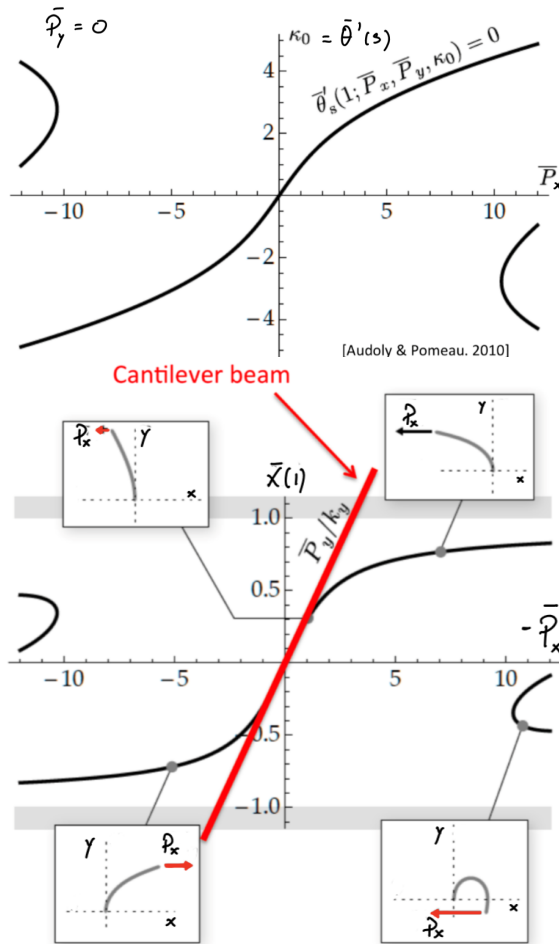


**Figure 3.8:** Example of nonlinear solutions of Euler's Elastica: pure transverse loading[Audoly and Pomeau, 2010]

In Fig. 3.9, the loading is directed along the vertical  $y$ -axis. In this case, as the compressive load increases (*i.e.* as  $\bar{P}_y$  takes negative values of increasing intensity), the straight solution loses its stability and buckling occurs; two new stable states emerge, where the beam is bent. Due to the symmetry of the problem, buckling can occur towards one side or the other. In physical buckling experiments, intrinsic defects like a small natural curvature of the beam or local material imperfections will influence to direction of buckling. This type of loss of stability through buckling is called a pitchfork bifurcation. Note that as the compressive load increases further, other (unstable) branches appear, corresponding to buckling of higher modes.

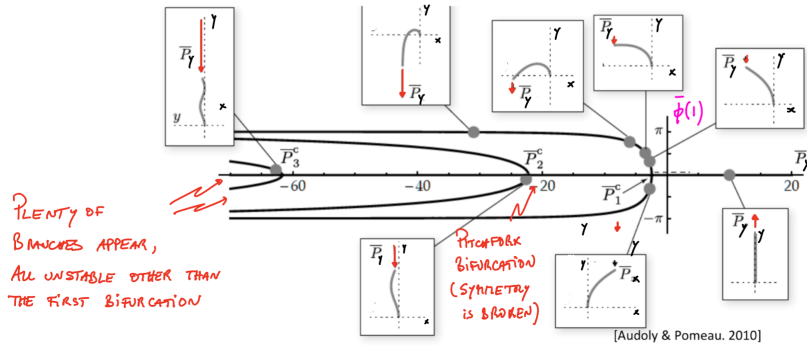


Figure 3.9: Example of nonlinear solutions of Euler's Elastica: pure axial loading. [Audoly and Pomeau, 2010]

### 3.6 Analytical methods to solve Euler's Elastica (elliptic integrals)

Before computational methods were widely available, one could still analytically compute shapes of beams undergoing large deformations, which is the topic of the last section of this chapter.

For simplicity, let us take  $P_x = 0, P_y = P$  and pinned ends. Moreover, we perform the following change of variables,  $\psi(s) = \theta(s) - \pi/2$ .

In that case, Euler's Elastica Equation becomes:

$$EI\psi'' + P \sin \psi = 0, \tag{3.72}$$

where  $0 \leq s \leq L$  and  $\theta'(0) = \theta'(L) = 0$ . Interestingly, if  $s$  were to be regarded as time, Eq. (3.72) would correspond exactly the equation for a pendulum. We will see that solutions can be expressed in terms of elliptic integrals. Integrating Eq. (3.72) yields:

$$\begin{aligned} \left(\frac{1}{2}EI\psi'^2 - P \cos \psi\right)' &= 0 \\ \Rightarrow \frac{1}{2}EI\psi'^2 - P \cos \psi &= C. \end{aligned} \tag{3.73}$$

Now, let  $\psi_0 \equiv \psi(0)$ , which is still an unknown, at this point. Note that  $\psi'(0) = 0$ . We thus get that:

$$\frac{1}{2}EI\psi'^2 - P \cos \psi = -P \cos \psi_0, \tag{3.74}$$

which leads to

$$\begin{aligned} \psi'^2 &= \left(\frac{2P}{EI}\right) (\cos \psi - \cos \psi_0) \\ \Rightarrow \psi' &= \pm \sqrt{\frac{2P}{EI}} \sqrt{\cos \psi - \cos \psi_0} \\ \Rightarrow \sqrt{\frac{2P}{EI}} s &= \int_{\psi}^{\psi_0} \frac{d\psi}{\sqrt{\cos \psi - \cos \psi_0}}. \end{aligned} \tag{3.75}$$

Note that the above result has been obtained by making no simplifying assumptions. This is an elliptic integral of first kind. We are looking for

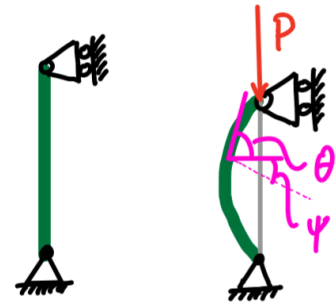


Figure 3.10: Problem we aim to solve analytically.

solutions with  $\psi_0 > 0$  that are symmetric with respect to the center of the column; *i.e.*,  $0 \leq s \leq \frac{L}{2} \Rightarrow \psi \geq 0$  and  $\psi' \leq 0$  with  $\psi(\frac{L}{2}) = 0$ .

Since  $\psi(\frac{L}{2}) = 0$ , we obtain

$$\sqrt{\frac{2P}{EI}} \frac{L}{2} = \int_0^{\psi_0} \frac{d\psi}{\sqrt{\cos \psi - \cos \psi_0}} = \sqrt{2} E_1 \left( \sin \frac{\psi_0}{2} \right), \quad (3.76)$$

where  $E_1$  is the complete elliptic integral of first kind. Eq. (3.76) establishes a relation between  $P$  and  $\psi_0$ .

When  $\psi_0 \ll 1$ , the above result simplifies to

$$\sqrt{\frac{2P}{EI}} \frac{L}{2} \approx \int_0^{\psi_0} \frac{d\psi}{\sqrt{\frac{\psi_0^2 - \psi^2}{2}}} = \frac{\pi}{\sqrt{2}}. \quad (3.77)$$

Therefore, the Euler buckling load is readily recovered as  $P_{cr} = \pi^2 EI/L^2$ , as we had derived earlier.

From the equations above, we can derive other quantities of interest, as follows:

- The deflection of center of the column  $\delta \equiv -x(\frac{L}{2})$  is

$$\frac{dx}{ds} = x' = \cos \theta = -\sin \psi, \quad (3.78)$$

and from above

$$\frac{d\psi}{ds} = \pm \sqrt{\frac{2P}{EI}} \sqrt{\cos \psi - \cos \psi_0}, \quad (3.79)$$

which yields

$$\frac{\delta}{L} = \frac{1}{L} \sqrt{\frac{EI}{2P}} \int_0^{\psi_0} \frac{\sin \psi d\psi}{\sqrt{\cos \psi - \cos \psi_0}}. \quad (3.80)$$

- The horizontal displacement  $\Delta \equiv L - y(L)$  through which the end load works is

$$\frac{\Delta}{L} = 1 - \frac{2}{L} \int_0^{\frac{L}{2}} \frac{dy}{ds} ds = 1 - \frac{2}{L} \sqrt{\frac{EI}{2P}} \int_0^{\psi_0} \frac{\cos \psi d\psi}{\sqrt{\cos \psi - \cos \psi_0}}. \quad (3.81)$$

These results are presented in Fig. 3.11.

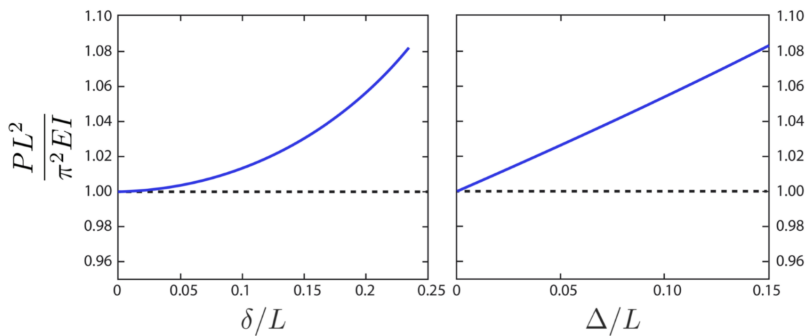


Figure 3.11: Elastica predictions.



## 4 Nonlinear Beam Theory

In this paragraph, we will expand both the linear beam theory and Euler's elastica that we developed in the previous two chapters, to allow us to consider 2D beam-like structures that may deform in a geometrically nonlinear way, potentially with finite strains and moderate rotations of the centerline. The goal is to obtain a general nonlinear beam theory, that may be reduced to the previous theories (*e.g.*, linear beams or Euler's elastica) in certain simplifying assumptions. We highlight that the general framework of the theory will be geometrically exact. This material was adapted from a sub-set of the lecture notes "Notes on Beams, Plates & Shells" by John W. Hutchinson, from a class entitled "Engineering Sciences 242r. Solid Mechanics: Advanced Seminar" that he used to teach at Harvard University (until 2012).

- 4.1 Strain-displacement relations for a nonlinear beam . . . . . 40
- 4.2 Simplifications of the general theory . . . . . 43
- 4.3 First-order constitutive relation for linear elastic behavior . . . . 46
- 4.4 Equations of equilibrium from variational methods . . . . . 46
- 4.5 Small strain, moderate rotation for circular rings . . . . . 48

### 4.1 Strain-displacement relations for a nonlinear beam

Let us consider the centerline of an elastic beam (in 2D). We take as convention that over-barred quantities correspond to the deformed configuration (blue line in Fig. 4.1) of this elastic beam. Since we are considering a line in space, at any point it is possible to attach a frame to the curve, in the form of a tangential vector  $\hat{\mathbf{t}}$  and a normal vector  $\hat{\mathbf{n}}$ . Also, we denote the displacement normal to the undeformed curve as  $w(s)$  and the displacement tangential to the undeformed curve as  $v(s)$ . These can be rigid body displacements, or differential displacements in the different directions, which will then be the source of strains and curvature that will build up as the beam deforms.

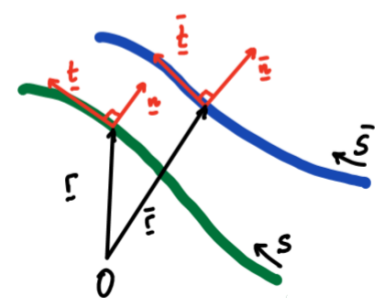


Figure 4.1: Centerlines of undeformed (green) and deformed (blue) configurations of a curvilinear beam (in 2D).

Based on the above definitions, the following kinematic relations of the following *deformed quantities* can be established, for  $\bar{\mathbf{r}}$ ,  $\bar{\mathbf{t}}$ , and  $d\bar{\mathbf{r}}/ds$ :

$$\bar{\mathbf{r}} = \mathbf{r} + w(s)\hat{\mathbf{n}} + v(s)\hat{\mathbf{t}}, \quad (4.1)$$

$$\bar{\mathbf{t}} = \frac{d\bar{\mathbf{r}}}{d\bar{s}} = \frac{d\bar{\mathbf{r}}}{ds} \frac{ds}{d\bar{s}}, \quad (4.2)$$

$$\frac{d\bar{\mathbf{r}}}{ds} = \frac{d\mathbf{r}}{ds} + \frac{dw}{ds}\hat{\mathbf{n}} + w\frac{d\hat{\mathbf{n}}}{ds} + \frac{dv}{ds}\hat{\mathbf{t}} + v\frac{d\hat{\mathbf{t}}}{ds}. \quad (4.3)$$

We also define the rotation,  $\varphi$ , as the angle between the undeformed and deformed configuration, as shown in Fig. 4.2,

$$\cos \varphi = \hat{\mathbf{t}} \cdot \bar{\mathbf{t}} = \hat{\mathbf{n}} \cdot \bar{\mathbf{n}} \quad (4.4)$$

and

$$\sin \varphi = \bar{\mathbf{t}} \cdot \hat{\mathbf{n}} = -\bar{\mathbf{n}} \cdot \hat{\mathbf{t}}. \quad (4.5)$$

The angular position of the tangent of the undeformed configuration is  $\psi$ , and that of the deformed configuration is  $\bar{\psi}$  (see Fig. 4.3). Consequently, the radius of curvature of the centerline in the undeformed configuration is,

$$\frac{1}{R(s)} = -\frac{d\psi}{ds}, \quad (4.6)$$

and the radius of curvature of the deformed centerline is,

$$\frac{1}{\bar{R}(\bar{s})} = -\frac{d\bar{\psi}}{d\bar{s}}. \quad (4.7)$$

From the above definitions, we get that

$$\frac{d\hat{\mathbf{n}}}{ds} = \frac{d\hat{\mathbf{n}}}{d\psi} \frac{d\psi}{ds} = -\hat{\mathbf{t}} \frac{d\psi}{ds} = \frac{1}{R} \hat{\mathbf{t}}, \quad (4.8)$$

and also

$$\frac{d\hat{\mathbf{t}}}{ds} = -\frac{1}{R} \hat{\mathbf{n}}. \quad (4.9)$$

Naturally, we find that  $\bar{\psi} = \psi + \varphi$ , or in words: the angular position of the tangent in the deformed configuration ( $\bar{\psi}$ ) equals that of the undeformed configuration ( $\psi$ ) plus the rotation ( $\varphi$ ).

From Eq. (4.3), we can now write the following expression:

$$\begin{aligned} \frac{d\bar{\mathbf{r}}}{ds} &= \hat{\mathbf{t}} + \frac{dv}{ds}\hat{\mathbf{t}} + \frac{w}{R}\hat{\mathbf{t}} + \frac{dw}{ds}\hat{\mathbf{n}} - \frac{v}{R}\hat{\mathbf{n}} \\ \Rightarrow \frac{d\bar{\mathbf{r}}}{ds} &= \hat{\mathbf{t}} \left( 1 + \frac{dv}{ds} + \frac{w}{R} \right) + \hat{\mathbf{n}} \left( \frac{dw}{ds} - \frac{v}{R} \right). \end{aligned} \quad (4.10)$$

Defining  $e \equiv \left( \frac{dv}{ds} + \frac{w}{R} \right)$  and  $\beta \equiv \left( \frac{dw}{ds} - \frac{v}{R} \right)$ , we can state that

$$\frac{d\bar{\mathbf{r}}}{ds} = \hat{\mathbf{t}}(1 + e) + \hat{\mathbf{n}}\beta. \quad (4.11)$$

The term  $e$  is a strain-like quantity related to displacements tangential to the curve. The quantity  $\beta$ , on the other hand, is related to displacements

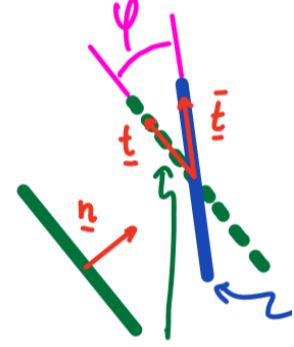


Figure 4.2: Angles for undeformed (green) and deformed (blue) centerlines.

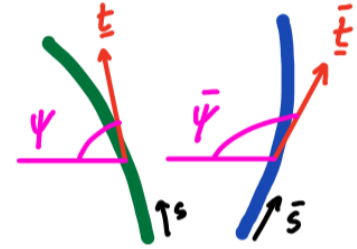


Figure 4.3: Angle  $\psi$  for undeformed (green) and deformed (blue) centerlines.

normal to the curve. Interestingly, not only displacements appear, but also the radius of curvature  $R$ .

We can get the following useful relation by the combination of Eqs. (4.2), (4.5) and (4.11):

$$\sin \varphi \equiv \bar{\mathbf{t}} \cdot \hat{\mathbf{n}} = \left( \frac{d\bar{\mathbf{r}}}{ds} \frac{ds}{d\bar{s}} \right) \cdot \hat{\mathbf{n}} = \beta \frac{ds}{d\bar{s}}. \quad (4.12)$$

Following the same procedure, we also write

$$\cos \varphi \equiv \bar{\mathbf{t}} \cdot \hat{\mathbf{t}} = \left( \frac{d\bar{\mathbf{r}}}{ds} \frac{ds}{d\bar{s}} \right) \cdot \hat{\mathbf{t}} = (1 + e) \frac{ds}{d\bar{s}}. \quad (4.13)$$

Let us define stretching strain as

$$\epsilon = \frac{d\bar{s}}{ds} - 1. \quad (4.14)$$

Using the trigonometric relation  $\cos^2 \varphi + \sin^2 \varphi = 1$ , Eqs. (4.12) and (4.13) yield

$$\begin{aligned} (1 + e)^2 \left( \frac{ds}{d\bar{s}} \right)^2 + \beta^2 \left( \frac{ds}{d\bar{s}} \right)^2 &= 1 \\ \frac{ds}{d\bar{s}} &= \left\{ (1 + e)^2 + \beta^2 \right\}^{-1/2} \\ \iff \frac{d\bar{s}}{ds} &= \left\{ (1 + e)^2 + \beta^2 \right\}^{1/2} \end{aligned} \quad (4.15)$$

Hence, we can write

$$\epsilon = \left\{ (1 + e)^2 + \beta^2 \right\}^{1/2} - 1 = \left\{ \frac{d\bar{\mathbf{r}}}{ds} \cdot \frac{d\bar{\mathbf{r}}}{ds} \right\}^{1/2} - 1. \quad (4.16)$$

We define the change of curvature  $\Delta\kappa$  as  $\Delta\kappa = (1/R - 1/\bar{R})$  with

$$\begin{aligned} \frac{1}{R} &= -\frac{d\psi}{ds} \\ \frac{1}{\bar{R}} &= \frac{d\bar{\psi}}{d\bar{s}} = -\frac{d\psi}{d\bar{s}} - \frac{d\varphi}{d\bar{s}} = -\frac{ds}{d\bar{s}} \left( \frac{d\psi}{ds} + \frac{d\varphi}{ds} \right), \end{aligned} \quad (4.17)$$

where we used the chain rule and the relations established before. Moreover, since from Eq. (4.14), we have  $\frac{d\bar{s}}{ds} = \epsilon + 1$ , we get

$$\begin{aligned} \Delta\kappa &= \frac{ds}{d\bar{s}} \left( \frac{d\psi}{ds} + \frac{d\varphi}{ds} \right) - \frac{d\psi}{ds} \\ &= (1 + \epsilon)^{-1} \left( \frac{d\varphi}{ds} \right) + \left( \frac{1}{1 + \epsilon} - 1 \right) \frac{d\psi}{ds}. \end{aligned} \quad (4.18)$$

Hence, the curvature-strain-rotation relation reads

$$\Delta\kappa = (1 + \epsilon)^{-1} \left[ \frac{d\varphi}{ds} + \frac{\epsilon}{R} \right]. \quad (4.19)$$

Thus far, we obtained a kinematics description for our nonlinear beam, with a geometrically-exact nonlinear strain-displacement relations. Still, it is useful to introduce an alternative stretching strain measure that is analogous to Lagrangian measure in 3D elasticity.

### 3D finite elasticity analogy

Recall from your previous Continuum Mechanics and Solid Mechanics classes that, often, we define the Green-St-Venant strain tensor as

$$\mathbf{E} = \frac{1}{2}(\mathbf{F}^T \mathbf{F} - \mathbf{I}), \quad (4.20)$$

where  $\mathbf{F} = dx/dX$  is the deformation gradient tensor and  $\mathbf{C} = \mathbf{F}^T \mathbf{F}$  is the Cauchy-Green deformation tensor ( $C_{ij} = F_{ki} F_{kj} = \frac{\partial x_k}{\partial X_i} \frac{\partial x_k}{\partial X_j}$ ).

Thus, we can define an alternative stretching strain as

$$\eta \equiv \frac{1}{2} \left[ \left( \frac{d\bar{s}}{ds} \right)^2 - 1 \right] = \frac{1}{2} ((\epsilon + 1)^2 - 1) = \frac{1}{2} \epsilon(2 + \epsilon) \quad (4.21)$$

or, alternatively, using the relations obtained before,

$$\eta = \frac{1}{2} \left[ \frac{d\bar{\mathbf{r}}}{ds} \cdot \frac{d\bar{\mathbf{r}}}{ds} - 1 \right] = e + \frac{1}{2} e^2 + \frac{1}{2} \beta^2. \quad (4.22)$$

Thus far, we have obtained exact equations for finite strain. We highlight that are not considering the curves to be inextensible, by contrast to what was done for Euler's Elastica (this was an over-simplification). As we shall see below, Euler's elastica can be regarded a special limit of the present theory.

## 4.2 Simplifications of the general theory

We now consider a variety of cases that the above geometrically exact kinematic description can reduce to under various approximations.

**Case A – Inextensible strains and finite rotations (*exact inextensionable theory*):** With the strain quantities  $e$  and  $\beta$  defined above, inextensibility implies that

$$\epsilon = \eta = 0, \quad (4.23)$$

which readily leads to

$$\sin \varphi = \beta, \quad (4.24)$$

$$e + \frac{1}{2} e^2 + \frac{1}{2} \beta^2 = 0, \quad (4.25)$$

and

$$\Delta \kappa = \frac{d\varphi}{ds}. \quad (4.26)$$

The above setting reduces to *Elastica* for originally straight elastic lines. Indeed,  $R \rightarrow \infty$  leads to

$$e = \frac{dv}{ds}, \quad (4.27)$$

and

$$\beta = \frac{dw}{ds} = \sin \varphi. \quad (4.28)$$

Using the fact that  $\cos^2 \varphi + \sin^2 \varphi = 1$ , Eq. (4.28) yields

$$\beta^2 = 1 - \cos^2 \varphi. \quad (4.29)$$

Going back to Eq. (4.25), we can write that

$$e + \frac{1}{2}e^2 + \frac{1}{2}(1 - \cos^2 \varphi) = 0, \quad (4.30)$$

which when solved gives

$$\cos \varphi = 1 + e = 1 + \frac{dv}{ds}. \quad (4.31)$$

To recover Euler's *Elastica*, we need to express the results obtained in Eqs. (4.28) and (4.31) in the variables we used when deriving *Elastica*'s equations, as shown in Fig. 4.4. Paying attention to the change of variables, we get that

$$x' = \frac{dw}{ds} = \sin \varphi, \quad (4.32)$$

and

$$y' = 1 - \frac{dv}{ds} = -\cos \varphi. \quad (4.33)$$

Since the angles were also defined differently, introducing  $-\varphi = \frac{\pi}{2} - \theta$ , we get back what we wrote in Chapter 3 for the kinematics of an inextensible, originally straight elastic curve (Euler's *Elastica*),

$$\begin{cases} x' = \sin \theta \\ y' = \cos \theta \\ \kappa = \frac{d\theta}{ds}. \end{cases} \quad (4.34)$$

**Case B – Small strains and finite rotations:** Small strains imply that  $|\epsilon| \ll 1$ , hence  $|\eta| \ll 1$ , thus  $\epsilon$  and  $\eta$  are of the same order. It can easily be shown that

$$\sin \varphi = \beta, \quad (4.35)$$

$$\epsilon = e + \frac{1}{2}e^2 + \frac{1}{2}\beta^2, \quad (4.36)$$

and

$$\Delta\kappa = \frac{d\varphi}{ds} + \frac{\epsilon}{R}. \quad (4.37)$$

**Small strains and small rotations:** This is the same situation as the beam theory developed in Chapter 1, except that now, we are also considering

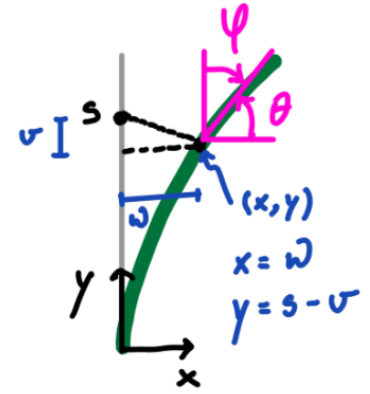


Figure 4.4: Deformed position of an originally straight beam.



naturally curved beams. This is a linear theory that can be obtained by linearizing the general theory obtained before. It can be shown that

$$\begin{aligned}\epsilon &= e = \frac{dv}{ds} + \frac{w}{R}, \\ \varphi &= \frac{dw}{ds} - \frac{v}{R}, \\ \Delta\kappa &= \left[ \frac{d\varphi}{ds} + \frac{\epsilon}{R} \right].\end{aligned}\quad (4.38)$$

**Case C – Small strains and moderate rotations:** The theory to describe the kinematics of a beam under small strains and moderate rotations will be investigated more in detail below. Indeed, it is acceptable to consider small strains when dealing with real cases, since most material only behave in a predictable manner up to a small percentage of strain. Intuitively, we also understand that if a beam is thin enough, it can undergo moderate rotations.

The assumption on strains leads to  $|\epsilon| \ll 1$ , and  $|\eta| \ll 1$ . On the other hand, the condition for moderate rotations is defined as  $\varphi^2 \ll 1$  (which is understandably less restrictive than  $\varphi \ll 1$ ).

It can be shown that  $\beta^2 \ll 1$  and therefore  $\varphi \approx \beta$ , recalling Eq. (4.35), and the Taylor expansion of a the sine function in the neighborhood of 0.

From Eq. (4.22), we get

$$\underbrace{\eta}_{\ll 1} = \underbrace{\epsilon}_{\ll 1} + \frac{1}{2}\epsilon^2 = e + \frac{1}{2}e^2 + \frac{1}{2}\underbrace{\beta^2}_{\ll 1}\quad (4.39)$$

which implies that

$$e + e^2 \ll 1. \quad (4.40)$$

Hence,  $e^2 \ll |e|$ . Summarizing all the results obtained thus far, we have

$$e = \frac{dv}{ds} + \frac{w}{R}, \quad (4.41)$$

$$\beta \approx \varphi = \frac{dw}{ds} - \frac{v}{R}, \quad (4.42)$$

$$\epsilon = e + \frac{1}{2}\varphi^2, \quad (4.43)$$

and

$$\Delta\kappa = \left[ \frac{d\varphi}{ds} + \frac{\epsilon}{R} \right]. \quad (4.44)$$

Interestingly, the only non-linearity is the  $\frac{1}{2}\varphi^2$  term in Eq. (4.43), arising from the fact that we are considering *moderate* rotations.

This case represents an important class of theories. It allows for rigorous buckling analyses for beams, columns and rings. Also, small strains and moderate rotations are the base assumption for some of the most widely used plate theories (e.g., von Karman).

### 4.3 First-order constitutive relation for linear elastic behavior

The scenario of *linear elastic behaviour* is relevant to many problems in structural mechanics, where bending and stretching strains are small, but rotations may be significant (we will make no assumptions on rotations).

We define  $B$  to be the bending stiffness and  $S$  to be the stretching stiffness of the beam. We also define  $\Phi(\Delta\kappa, \epsilon)$  as the energy density function (per unit length), which is a function of the change of curvature  $\Delta\kappa$  and the strain  $\epsilon$ , because bending and stretching are the two ways to store elastic energy in the structure. In this framework, the bending moment (per unit length) is

$$M = \frac{\partial\Phi}{\partial\Delta\kappa}, \quad (4.45)$$

and the stretching force (per unit length) is

$$F = \frac{\partial\Phi}{\partial\epsilon}. \quad (4.46)$$

The above results are reasonable since, for a linear elastic straight beam,

$$\Phi_A = \frac{1}{2}B\Delta\kappa^2 + \frac{1}{2}SE^2 \Rightarrow \begin{cases} M = \frac{\partial\Phi_A}{\partial\Delta\kappa} = B\Delta\kappa \\ F = \frac{\partial\Phi_A}{\partial\epsilon} = S\epsilon. \end{cases} \quad (4.47)$$

Instead of  $(\Delta\kappa, \epsilon)$  as pair of strain measures, we can alternatively use  $(K, \epsilon)$ , with  $K = \Delta\kappa - \frac{\epsilon}{R}$ . Since stretching strains are small,  $\epsilon \ll 1$  and Eq. (4.44) becomes

$$K = \frac{d\varphi}{ds}. \quad (4.48)$$

Hence, instead of  $\Phi_A$ , we can use  $\Phi_B = \frac{1}{2}BK^2 + \frac{1}{2}SE^2$ . Hence,

$$\begin{cases} M = \frac{\partial\Phi_B}{\partial K} = BK \\ F = \frac{\partial\Phi_B}{\partial\epsilon} = S\epsilon \end{cases} \quad (4.49)$$

The two expressions for  $M$  and  $F$  now look similar. Note that, even if  $K$  is a *curvature-like quantity*, it does not necessarily correspond to the curvature of the beam. Also, note that for flat beams, using  $\Phi_A$  or  $\Phi_B$  is identical; this is not the case for naturally curved beams. The expression of  $\Phi_B$  is easier to handle, as it is more intuitive. We will be able to derive the 1D theory based solely on the deformation of the neutral axis.

### 4.4 Equations of equilibrium from variational methods

We will focus on the theory that considers small strains and moderate rotations<sup>1</sup>. Recalling Eqs. (4.41) to (4.44), the expressions for virtual

1: As illustration, we could have followed one of the other theories.

displacements and rotations are written as

$$\delta\epsilon = \delta e + \delta\bar{\varphi}, \quad (4.50)$$

$$\delta K = \frac{d\delta\varphi}{ds}, \quad (4.51)$$

$$\delta e = \frac{d\delta v}{ds} + \frac{\delta w}{R}, \quad (4.52)$$

and

$$\delta\varphi = \frac{d\delta w}{ds} - \frac{\delta v}{R}. \quad (4.53)$$

The principle of virtual work (POVW) states that the internal work (IVW) exerted by the internal forces and moments has to equal the external virtual work (EVW) by external forces, for all kinematically admissible virtual displacements  $\delta v$  and  $\delta w$ . As we saw in Chapter 3, this statement is identical to writing that the first variation of the total energy has to equal zero.

Integrating from the start to the end of the curve, we obtain the internal virtual work as

$$IVW = \int_0^L (M\delta K + F\delta\epsilon) ds, \quad (4.54)$$

and the external virtual work

$$EVW = \int_0^L (p_n\delta w + p_t\delta v) ds + [P_n\delta w + P_t\delta v + m\delta\varphi]_0^L. \quad (4.55)$$

In Eq. 4.55, we considered the distributed loads  $p_n$  and  $p_t$  along the beam, respectively in the normal and tangential direction to the curve. In addition, we used point loads or moments at the edges of the beam;  $P_n$  and  $P_t$  are the point loads in the normal and tangential direction respectively, and  $m$  is the point moment.

Expanding Eq. (4.54) and integrating by parts, we get that

$$\begin{aligned} IVW &= \int_0^L \left( M \frac{d}{ds} \left( \frac{d\delta w}{ds} - \frac{\delta v}{R} \right) + F \left( \frac{d\delta v}{ds} + \frac{\delta w}{R} + \varphi \left( \frac{d\delta w}{ds} - \frac{\delta v}{R} \right) \right) \right) ds \\ &= \int_0^L \left[ \left( \frac{d^2 M}{ds^2} + \frac{F}{R} - \frac{d(F\varphi)}{ds} \right) \delta w + \left( \frac{1}{R} \frac{dM}{ds} - \frac{dF}{ds} - \frac{F\varphi}{R} \right) \delta v \right] ds \\ &\quad + \left[ M \frac{d\delta w}{ds} + \left( -\frac{dM}{ds} + F\varphi \right) \delta w + \left( -\frac{M}{R} + F \right) \delta v \right]_0^L. \end{aligned} \quad (4.56)$$

Now, enforcing the POVW,  $IVW = EVW$  (i.e.,  $\delta U_{\text{tot}} = 0$ ), we finally get

$$\begin{cases} \frac{d^2 M}{ds^2} + \frac{F}{R} - \frac{d(F\varphi)}{ds} = p_n \\ \frac{1}{R} \frac{dM}{ds} - \frac{dF}{ds} - \frac{F\varphi}{R} = p_t, \end{cases} \quad (4.57)$$

with the conditions at the boundaries

$$\begin{aligned} & \left[ M \frac{d\delta w}{ds} + \left( -\frac{dM}{ds} + F\varphi \right) \delta w + \left( -\frac{M}{R} + F \right) \delta v \right]_0^L \\ & = \left[ m \frac{d\delta w}{ds} + P_n \delta w + \left( P_t - \frac{m}{R} \right) \delta v \right]_0^L. \end{aligned} \quad (4.58)$$

At either end, boundary conditions thus involve specification of

$$\begin{cases} M = m & \text{or } \frac{dw}{ds} \\ -\frac{dM}{ds} + F\varphi = P_n & \text{or } w \\ \frac{M}{R} - F = \frac{m}{R} - P_t & \text{or } v \end{cases} \quad (4.59)$$

## 4.5 Small strain, moderate rotation for circular rings

*Important note:* When the distributed loads per unit length,  $p_n$  and  $p_t$ , are written with respect to the undeformed configuration, *i.e.*, when they act along the reference  $\hat{\mathbf{t}}$  and  $\hat{\mathbf{n}}$ , we call them **dead loads**. By contrast, pressure loading, *real pressure*, is defined as load per unit length acting parallel to  $\bar{\mathbf{n}}$  (normal vector of the *deformed* centerline), and is an example of a **live load**.

Let us consider a naturally curved ring onto which we apply an external pressure; the geometry of this ring is presented in Fig. 4.5. Our task is to determine when it will buckle under pressure loading. In this task, we will need to specialize Eqs. (4.57) for a ring geometry.

First, we write the arclength along the ring,  $s = R\theta$ , hence  $ds = R d\theta$ , where the azimuthal angle,  $\theta$ , is measured in the undeformed configuration. We will assume linearly elastic isotropic material properties, such that  $M = BK$  and  $F = S\epsilon$ . From Eq. (4.41), we obtain

$$\varphi = \frac{dw}{ds} - \frac{v}{R} \Rightarrow \varphi = \frac{w' - v}{R}, \quad (4.60)$$

and from Eq. (4.42)

$$e = \frac{dv}{ds} - \frac{w}{R} \Rightarrow e = \frac{v' + w}{R}, \quad (4.61)$$

where priming a variable means differentiation with respect to  $\theta$ .

Specializing Eqs. (4.57) and writing them as a function of  $\varphi$  and  $e$  as derived in Eqs. (4.60) and (4.61) above, yields

$$\begin{aligned} B\varphi''' + SR^2 \left( e + \frac{1}{2}\varphi^2 \right) - SR^2 \left[ \left( e + \frac{1}{2}\varphi^2 \right) \varphi \right]' &= R^3 p_n \\ B\varphi'' - SR^2 \left( e + \frac{1}{2}\varphi^2 \right) - SR^2 \left( e + \frac{1}{2}\varphi^2 \right) &= R^3 p_t \end{aligned} \quad (4.62)$$

The boundary conditions depend on whether the ring is complete, and how it is supported.

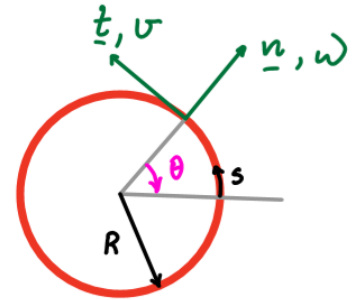


Figure 4.5: Circular ring of radius  $R$ .

**Classical buckling of circular ring under uniform radial (dead) pressure<sup>2</sup>** : We now consider that both the ring geometry and the radial pressure are axisymmetric. We can easily check that Eq. (4.62) admits the solution

$$\begin{cases} w = w_0 = -\frac{pR^2}{S} \\ v = 0, \end{cases} \quad (4.63)$$

and

$$\begin{cases} e = e_0 = \frac{w_0}{R} \\ \varphi = 0. \end{cases} \quad (4.64)$$

This solution is similar to a straight solution in the Euler buckling case. We thus want to know when this solution loses stability, and a new solution arises, corresponding to buckling.

**Buckling analysis:** For a specified load  $p$ , we will perturb the base solution ( $w$  around  $w_0$  and  $v$  around 0) with  $\mu$  as a perturbation parameter. We can write

$$\begin{cases} w = w_0 + \mu w_1 + \dots \\ v = 0 + \mu v_1 + \dots \end{cases} \quad (4.65)$$

and

$$\begin{cases} \varphi = 0 + \mu \varphi_1 + \dots = 0 + \mu \frac{(w'_1 - v_1)}{R} \\ e = e_0 + \mu e_1 + \dots = e_0 + \mu \frac{(v'_1 + w_1)}{R} \end{cases} \quad (4.66)$$

Substituting Eqs. (4.65) and (4.66) into the fully nonlinear governing Eqs. (4.62) and linearizing them with respect to  $\mu$  (*i.e.*, only considering first order terms), we get

$$\begin{cases} B\varphi_1''' + SR^2e_1 + pR^3\varphi_1' = 0 \\ B\varphi_1'' - SR^2e_1' + pR^3\varphi_1 = 0. \end{cases} \quad (4.67)$$

We can eliminate  $e_1$  by differentiating the first equation and by adding it to the second. We finally get the eigenvalue problem

$$B(\varphi_1'''' + \varphi_1'') + pR^3(\varphi_1'' + \varphi_1) = 0, \quad (4.68)$$

with  $p$  as the eigenvalue. We are looking for eigenmodes such that  $\varphi_1 = \sin(n\theta)$  or  $\varphi_1 = \cos(n\theta)$  for  $n$  an integer. Substituting a sinusoidal function for  $\varphi_1$ , we obtain,

$$p_n = \frac{B}{R^3}n^2. \quad (4.69)$$

In addition, the second equation of Eqs. (4.67) yields the relation

$$e_1' - \frac{R}{S} \left( \frac{B\varphi_1''}{R^3} + p\varphi_1 \right) = 0, \quad (4.70)$$

for all  $n$ , which is also an eigenvalue problem. Indeed, since

$$e_1 = \frac{v'_1 + w_1}{R}, \quad (4.71)$$

$$2: \begin{cases} p_n \equiv -p \\ p_t = 0 \end{cases}$$

and

$$\varphi_1 = \frac{w_1' - v_1}{R}, \quad (4.72)$$

we can solve Eq. (4.70) by using sinusoidal functions for  $w_1$  and  $v_1$ :

$$\begin{cases} w_1 = w_1^0 \cos(n\theta) \\ v_1 = v_1^0 \sin(n\theta). \end{cases} \quad (4.73)$$

We can then write the amplitude of the modes:

$$\begin{cases} v_1^0 n + w_1^0 = 0 \\ v_1^0 + n w_1^0 = -R. \end{cases} \quad (4.74)$$

For  $n = 1$ , there is no solution<sup>3</sup>. The lowest eigenvalue corresponds to  $n = 2$ , and leads to the critical buckling pressure  $p_c$ . Thus, we finally get that for dead pressure

3:  $v_1^0 + w_1^0 = 0$  and  $v_1^0 + w_1^0 = -R$ , which is not possible.

$$\begin{aligned} p_c &\equiv p_2 = \frac{4B}{R^3} \\ w_1^0 &= -\frac{2R}{3} \\ v_1^0 &= \frac{R}{3}. \end{aligned} \quad (4.75)$$

Finally, note that  $e_1 = 0$ , hence for  $n = 2$  the buckling mode is inextensible to the first order.

**Same ring problem but with live pressure:** The live pressure is  $-p\bar{\mathbf{n}}$  and the external virtual work is therefore written as

$$EVW = - \int p\bar{\mathbf{n}} \cdot (\delta w\hat{\mathbf{n}} + \delta v\hat{\mathbf{t}})d\bar{s}. \quad (4.76)$$

From the nonlinear strain-displacement relations above, we know

$$\bar{\mathbf{t}} = \frac{ds}{d\bar{s}} ((1+e)\hat{\mathbf{t}} + \beta\hat{\mathbf{n}}), \quad (4.77)$$

hence

$$\bar{\mathbf{n}} = \frac{ds}{d\bar{s}} (-\beta\hat{\mathbf{t}} + (1+e)\hat{\mathbf{n}}). \quad (4.78)$$

The external virtual work is therefore

$$EVW = - \int p[(1+e)\delta w - \beta\delta v]ds. \quad (4.79)$$

If we now revisit Eqs. (4.57), but with external virtual work for live pressure, we can show that

$$\begin{aligned} B\varphi''' + SR^2 \left( e + \frac{1}{2}\varphi^2 \right) - SR^2 \left[ \left( e + \frac{1}{2}\varphi^2 \right) \varphi \right]' &= -R^3 p \\ B\varphi'' - SR^2 \left( e + \frac{1}{2}\varphi^2 \right) - SR^2 \left( e + \frac{1}{2}\varphi^2 \right) &= R^3 \varphi p, \end{aligned} \quad (4.80)$$

where we simplified  $-R^3(1+e)p = -R^3p$  since  $e \ll 1$ .

The axisymmetric, pre-buckled solution will be the same as that for the dead pressure case,

$$\begin{cases} w = w_0 \\ v = 0 \end{cases} \quad (4.81)$$

where  $w_0$  is independent of  $\theta$ . The variables  $e$  and  $\varphi$  are given by

$$\begin{cases} e = \frac{dv}{ds} - \frac{w}{R} \Rightarrow e = -\frac{w_0}{R} \\ \varphi = \frac{dw}{ds} - \frac{v}{R} \Rightarrow \varphi = 0. \end{cases} \quad (4.82)$$

Inserting this into Eqs. (4.80), we get

$$\begin{cases} SR^2e = -R^3p \\ e_0 = -\frac{pR}{S} \end{cases} \Rightarrow w_0 = \frac{-pR^2}{S} \quad (4.83)$$

which is the same solution as for the dead pressure case.

For the buckling analysis, we linearize Eqs. (4.80) as before to obtain

$$\begin{cases} B\varphi'''' + SR^2e_1 + pR^3\varphi_1' = 0 \\ B\varphi_1'' - SR^2e_1' = 0 \end{cases} \quad (4.84)$$

Differentiating the first equation and summing it with the second, we get

$$B(\varphi_1'''' + \varphi_1'') + pR^3\varphi_1'' = 0. \quad (4.85)$$

We are looking for solutions of the form  $\varphi_1 = \varphi_1^0 \cos(n\theta)$ . Replacing this into Eq. (4.85), we obtain

$$p = \frac{B}{R^3} (n^2 - 1) \quad (4.86)$$

for  $n=0, 1, 2, \dots$

- ▶  $n = 0$  is not a solution since the only axisymmetric solution is the pre-buckling solution.
- ▶  $n = 1$  is not a solution except for potential rigid body motion, which are nonetheless not allowed due to pre-buckling axisymmetry.
- ▶ The lowest eigenvalue and therefore lowest buckling pressure is therefore, for  $n = 2$ ,

$$p_c^l = \frac{3B}{R^3} \quad (4.87)$$

which is 25% lower than for the dead pressure case (where  $p_c^d = \frac{4B}{R^3}$ ).

The difference for the critical buckling pressure between the cases of dead pressure and the more realistic live pressure is significant. First, this difference highlights the importance of *keeping track* of the deformed configuration and, hence, the value of the formalism developed in this chapter. Secondly, from a more practical stand-point, it is important to note that the more realistic scenario of live pressure yields a lower value of  $p_c$ . In an engineering setting, had we taken the dead pressure approach, the structure could buckle in reality prior to the (simplified) prediction,

potentially with catastrophic results. Recognizing the important consequences between dead or live pressure loadings is important in structural mechanics. Finally, we also note that, by contrast to nonlinear beams, the buckling of shells is insensitive to the difference between dead versus live pressure loading, as we will see towards the end of this course.